

**SYNTHESIS, CHARACTERIZATION OF ZnO NANO PHOTOCATALYSTS
AND THEIR APPLICATION IN PHOTOREMEDIATION OF WASTE WATER**

BY

LUCY JEPCHIRCHIRCHEBOR

**RESEARCH THESIS SUBMITTED TO THE SCHOOL OF SCIENCE IN
PARTIAL FULFILLMENT OF THE REQUIREMENT FOR DEGREE OF
MASTER OF SCIENCE IN INORGANIC CHEMISTRY, UNIVERSITY OF
ELDOROT, KENYA**

AUGUST, 2015

DECLARATION

Declaration by the Student

This thesis is my original work; it has not been presented for a degree in any other university. No part of this thesis may be reproduced without prior knowledge of the author or University of Eldoret.

Signature..... Date.....

Name: Lucy JepchirchirChebor

Reg No:SC/PGC/001/011

Declaration by the Supervisors

This thesis has been submitted for examination with our approval as university supervisors.

Signature..... Date.....

Prof. LuswetiKituyi

University of Eldoret

Signature..... Date.....

Dr. Dickson Andala

MultimediaUniversity Nairobi

DEDICATION

To my children Meshack, Abeland Faith, May you live to realize your dreams and aspirations and inherit the peace, love and prosperity that the world has to offer.

ABSTRACT

Water scarcity and its contamination with toxic metal ions and organic dyes represent a serious worldwide problem in the 21st century. Today's world faces alarming challenges in the rising demand for drinking water and conditions are particularly bad in developing countries with the rapid escalation of industrialization towards a developed society. The waste products generated from the textiles, chemicals, mining and metallurgical industries are mainly responsible for contaminating the water. This contaminated water contains non-biodegradable effluents such as heavy metal ions (Copper, Nickel, Cadmium, Arsenic etc.) and organic materials such as dyes that are carcinogenic to human beings and harmful to the environment because of their bioaccumulation, non-biodegradable property and toxicity even at low concentrations. In an effort to reduce the environmental effects of heavy metals and dyes, various techniques have been employed. However, these techniques are expensive and ineffective resulting in an intensively coloured discharge and high concentration of heavy metals from the treatment facilities. Nanotechnology is a promising field in waste water treatment. This study aimed at assessing the efficiency of synthesized ZnO nanoparticles in photodegradation of synthetic dyes and adsorption of heavy metal ions from waste water. The objectives of this study were to synthesize ZnO nanoparticles, characterize and apply it in adsorption of heavy metals and photodegradation of methyl orange dye. Methyl orange was used as a model dye and the heavy metal determined were Ni^{2+} , Cd^{2+} and Cu^{2+} . Precipitation technique was used to synthesize ZnO nanoparticles. Two samples L_1 and L_2 were synthesized. They were characterized using PXRD (Power X-ray Diffraction), FTIR (Fourier Transform Infra-Red), SEM (Scanning Electron Microscopy) and EDX (Energy Dispersive X-ray Spectroscopy), methods of analysis. Photodegradation studies were carried out using solar and fluorescent light energy. The EDX results showed elemental composition of ZnO nanoparticles which showed 54.00% Zn, 44.07% O and 1.93% Mn impurities for L_1 and 55.34% Zn, 42.3% O and 2.37% Mn impurities for L_2 . The PXRD results showed diffraction peaks which were indexed to ZnO reference as per JCPDS file 80-0075. The average size of ZnO nanoparticles was found to be 26 nm. FTIR spectra showed a broad band at around 430 cm^{-1} with shoulder shape, characteristics of Zn-O bond. The images obtained by SEM showed rod shaped clusters of nanoparticles. They were distributed well within a range of 100 nm which is a favorable property to exhibit better photo catalytic activity. The results of heavy metal ions adsorption showed an increase in percentage removal with increase in adsorbent dose and contact time. There was a decrease with increase in heavy metal concentration (ppm). For photodegradation, the results indicated an increase in colour removal with increase in photocatalyst dose and contact time and a decrease with increase in concentration of methyl orange. In conclusion, ZnO nanoparticles used as an adsorbent and a photocatalyst is efficient and a promising technique for treatment of waste water from textile, paper and dyeing industry and metallurgical industries. It can act as an adsorbent for heavy metal ions and a photocatalyst for degradation of synthetic dyes. Future studies could focus on possibilities of improving and commercializing this material through designing a treatment facility that incorporates it, with the aim of being used on large scale waste water treatment.

TABLE OF CONTENTS

DECLARATION	i
DEDICATION	ii
ABSTRACT	iii
LIST OF FIGURES	ix
LIST OF ABBREVIATIONS	xii
ACKNOWLEDGEMENT	xv
CHAPTER ONE	1
INTRODUCTION	1
1.1 Background Information.....	1
1.1.1 Environmental Potentials of Nano Technology	3
1.2 Problem Statement	5
1.3 Justification	7
1.4 Objectives	8
1.4.1 General Objective	8
1.4.2 Specific Objectives	8
1.5 Research questions.....	8
CHAPTER TWO	10
LITERATURE REVIEW	10
2.1 Synthesis of ZnO nanoparticles	10
2.2 Structural Characterization of Nanoparticles.....	10
2.2.1 XRD (X-ray diffraction)	11
2.2.2 Powder diffraction	11
2.2.3 Fourier Transform Infrared Spectroscopy (FTIR)	14

2.2.4 Energy dispersive X-ray Spectroscopy (EDX)	15
2.2.5 Scanning Electron Microscope (SEM)	16
2.3 Nano-Materials and their Environmental Applications	17
2.4 Application of Nanotechnology in Water and Wastewater Treatment	21
2.5 Photo-catalytic Degradation of Dyes	22
2.6 Dye Photo-catalytic degradation Mechanism	23
2.7 Health Effects of heavy metals	25
2.8 The use of metal oxides nanoparticle as heavy metals adsorbent in waste water	27
2.11 Stabilizing agents	31
2.12 Related studies	32
2.13 Adsorption Isotherms for the photocatalytic degradation of dye	35
CHAPTER THREE	37
MATERIALS AND METHODS	37
3.1 Research approach	37
3.2 Materials and Reagents	37
3.3 Synthesis of ZnO nanoparticles	37
3.4 Characterization of ZnO nanoparticles particles	39
3.5 Heavy metal analysis	39
3.5.1 Optimizing operating conditions	39
3.5.2 Calibration Curves	41
3.5.3 Laboratory-based heavy metals analysis	41
3.6 Photo-catalytic degradation studies	42

3.6.1 Preparation of dye solution	42
3.6.2 Measurement of concentration of dye solution.....	43
3.6.3 Determination of extent of removal of the dye	43
3.7 Factors that govern degradation process.....	44
3.7.1 Effect of variation of initial concentration of MeO dye	44
3.7.2 Effect of variation of dose of photo catalyst on photo degradation of MeO	44
3.7.3 Effect of variation of contact time on the photo-degradation of MeO	45
CHAPTER FOUR.....	46
RESULTS AND DISCUSSION	46
4.1 Characterization of ZnO nanoparticles particles.....	46
4.2 Powder X-Ray Diffraction (PXRD).....	46
4.3 SEM Analysis	53
4.4 EDX Analysis	56
4.5 Heavy Metals Analysis	58
4.5.1 Effect of initial heavy metals concentration on Adsorption capacity of ZnO nanoparticles	58
4.5.2 Effect of adsorbent dose on percentage removal of heavy metals.....	59
4.5.3 Effect of pH on Heavy Metal adsorption.....	61
4.6 Photo-catalytic degradation studies	64
4.6.1 Effect of variation of initial concentration of dye on photo degradation of methylo range dye.....	66
4.6.2 Effect of variation of dose of photocatalyst (L ₁ and L ₂) on photo degradation of MeO dye	67

4.6.3 Effect of variation of contact time on photo degradation of MeO dye	70
4.7 Equilibrium isotherm models for photo degradation of MeO dye using sunlight.....	71
4.8 Equilibrium isotherm models for photo degradation of MeO dye using florescent	73
4.9 Adsorption kineticsfor photo degradation of MeO dye using sunlight.....	75
4.10 Adsorption kineticsfor photo degradation of MeO dye using florescent.....	77
4.11 Comparison of Adsorption Efficiency of ZnO nanoparticles	80
CHAPTER FIVE	81
CONCLUSION AND RECOMMENDATIONS.....	81
5.1 Conclusion	81
5.2 Recommendations.....	82
REFERENCES.....	83
APPENDICES.....	91

LIST OF TABLES

Table 3.1: Optimized conditions for AAS	41
Table 4.1: Effect of variation of initial concentration of dye on photo degradation of methyl orange dye.....	66
Table 4.2: Effect of variation of dose of photo catalyst (L_1 and L_2) on photo degradation of MeO dye	69
Table 4.3: Effect of variation of contact time on photo degradation of MeO dye.....	70

LIST OF FIGURES

Figure 2. 1: Reflection of incident monochromatic X-ray from successive planes of crystal lattices.....	13
Figure 2. 2: Summary of photo-catalytic degradation of dyes.....	25
Figure 4.1: Observed Powder XRD pattern.....	47
Figure 4.2: Reference JCPDS file 80-0075 for Wurzite ZnO.....	48
Figure 4.3: Observed FTIR pattern.....	51
Figure 4.4: Reference ZnO Spectra	52
Figure 4.5: L ₁ SEM diagram (Magnification = 80.39K X).....	53
Figure 4.6: L ₂ SEM diagram (Magnification = 80.68K X).....	54
Figure 4.7: EDX Pattern ZnO L ₁	56
Figure 4.8: EDX Pattern ZnO L ₂	57
Figure 4.9: Effect of initial heavy metals concentration on adsorption capacity of ZnO nanoparticles	59
Figure 4.10: Effect of adsorbent dose on percentage removal of heavy metals	60
Figure 4.11: Effect of pH on ZnO nano particles heavy metals adsorption	62
Figure 4.12: Standard curve for Methyl Orange dye	64
Figure 4.13: Langmuir adsorption isotherm of Methyl Orange adsorption.....	71
Figure 4.14: Freundlich adsorption isotherm of methyl orange adsorption.....	72
Figure 4. 15: Langmuir Isotherm for photo degradation of MeO dye using florescent.....	73
Figure 4. 16: Freundlich Isotherm for photo degradation of MeO dye using fluorescent	74

Figure 4.17: Lagergren first order plot of methyl orange degradation under sunlight	75
Figure 4.18: Lagergren second order plot of methyl orange degradation under sunlight.....	76
Figure 4. 19: Lagergren first order plot of methyl orange adsorption under fluorescent illumination	78
Figure 4. 20: Lagergren second order plot of methyl orange adsorption under fluorescent illumination.....	79

LIST OF APPENDICES

Appendix I: Effect of variation of contact time on photodegradation of MeO dye under sunlight.....	91
Appendix II: Effect of variation of contact time on photodegradation of MeO dye under fluorescent.....	91
Appendix III: Adsorption Isotherms Data (Under Sunlight)	92
Appendix III: Adsorption Isotherms Data (Under Fluorescent Light)	93
Appendix IV: Effect of adsorbent dose on percentage removal of heavy metals.....	94
Appendix V: Effect of initial concentration of heavy metals	94
Appendix VI: Effect of pH	94
Appendix VII: Lagergren Adsorption Kinetics Data (Under Sunlight).....	95
Appendix IX: Lagergren Adsorption Kinetics Data (Under Fluorescent).....	95
Appendix X: Observed SEM diagram ZnO nanorods, L ₁ at low magnification (Mag 20.59 K)	96
Appendix XI: Observed SEM diagram L ₂ at Low Magnification (Mag 20.66 K)	97

LIST OF ABBREVIATIONS

AAS	Atomic Absorption Spectrometer
AFM	Atomic Force Microscopy
AOP	Advanced Oxidation Processes
BDH	Burrell Durrant Hifle
BET	Brunauer–Emmett–Teller
eCB	electron conduction band
ED	Energy Dispersive
EDX	Energy Dispersive X-ray Spectroscopy
EHT	Extra High Tension
EXAFS	Extended X-ray Absorption Fine Structure
FTIR	Fourier Transform Infrared Spectroscopy
FWHM	Full Width at Half Maximum
FWHM	Full-Width Half-Maximum
hVB	hole valence band
IBM	International Business Machines

ICRAF	International Center for Research in Agroforestry
IR	Infra Red
JCPDS	Joint Committee on Powder Diffraction Standards
MBE	Molecular Beam Epitaxy
OD	Optical Density
PXRD	Powder X-ray Diffraction
PZC	Point of Zero Charge
QSAR	Quantitative Structure–Activity Relationship
SDD	Silicon Drift Detectors
SDD	Silicon Drift Detectors
SEM	Scanning Electron Microscope
SPM	Scanning Probe Microscopy
SSA	Specific Surface Area
STM	Scanning Tunneling Microscope
TEM	Transmission Electron Microscopy

USEPA	US Environmental Protection Agency
UV-VIS	UV-Visible Spectroscopy
WDS	Wavelength-dispersive spectroscopy
WDS	Wireless Distribution System
WHO	World Health Organization
XRD	X-Ray Diffraction

ACKNOWLEDGEMENT

The success of this project is highly indebted to the efforts and willingness of many. First, to the Almighty God for good health and preservation during the entire duration of the project. My appreciation goes to my supervisors; Prof. Lusweti of University of Eldoret and Dr Andala from Kenyatta University for supervisory work and assisting me in analysis using methods that were not found within the country. May the Lord crown their efforts with more strength and wisdom.

I also acknowledge the efforts of Mr Bartilol from the Department of Nuclear Science, University of Nairobi who assisted me in finding PXRD and FTIR instrumentation at ICRAF Nairobi and Mr Maina who continuously pointed out areas that needed corrections in the project.

The entire family of Mr and Mrs Chebor deserves a mention for their unceasing moral and material support in my life. I too wish to most sincerely thank my husband Patrick for typing, printing and binding the project. Indeed he means a lot to me.

CHAPTER ONE

INTRODUCTION

1.1 Background Information

Dyes are an important class of synthetic organic compounds used in textile industry, paper, dyeing and plastic industries as colour for dyeing their products. A huge amount of water is used which results in production of dye containing water. These industries use approximately 10,000 dyes and pigments (Baouer *et al.*, 2001). Metal processing waste water often contains species of heavy metals for example Cr (IV), etc which are toxic and could act as carcinogens, terratogens and mutagens in biological systems. Industries are supposed to reduce the chromium in their effluents to around 0.1mg/L, before discharging it into the sewer system (Ayuso *et al.*, 2003).

“Nano “is derived from the Greek word for dwarf. A nanometer is one billionth of a meter (10^{-9}) and might be represented by the length of ten hydrogen atoms lined up in a row. It emerged billions of years ago at the point where molecules began to arrange in complex forms and structures that launched life on earth. Through evolution, mutations and adaptations; plants were able to carry out photosynthesis (Roco, 1999). Another example of a natural nanotechnology is “chemical catalysis “through catalysts called enzymes which sometimes are considered as indispensable for completion of some chemical reactions (Akohe *et al.*, 2007). Nanostructure science and technology is a broad

research area that encompasses the creation of new materials from nanosized building blocks (Hu and Shaw,1998).

Nanotechnology was first proposed, by the Nobel Prize winning physicist Richard Feynman, who suggested that someday it would be possible to put the entire 24 volume Encyclopedia Britannica on the head of a pin(Feynman, 1959). Feynman proposed that tiny robots might be able to build chemical substances. He noted that they could be used to create nano-machines. He had also pointed out that a new class of miniaturized instruments would be needed to manipulate and measure the properties of the small "nano" structures.

In the 1980's these instruments were invented, they could begin to do what Feynman talked about. However, little happened until researcher Drexler, the name that is most widely seen in nano-technological circles, released his book Engines of Creation (Drexler, 1986). This book engines of creation, created a sensation for its depiction of magnificent control over matter. The book also describes self-replicating nano-machines that could produce virtually any material good, while reversing the global warming, curing disease and dramatically extending the lifespan. He has also authored a number of technical journal articles and books on the subject including and in bounding the future, the nanotechnology revolution (Keiper, 2003). In both books, Drexler proposed a number of potential benefits of this new technology. He has also pointed out the potential hazards of molecular manipulation, some of which are unpredictable. His books emerged as the main

driving force among the research communities. For instance, the following is one of the examples of technique demonstrated by IBM researchers. The technique of manipulation of atoms was first demonstrated, when in April 1990, a team in the IBM research division placed thirty-five xenon atoms in a precise pattern and spelled out the letters "IBM. The logo is 60 billionths of an inch wide, or 13 millionths of the diameter of a human hair (IBM Corporation, 2001).

1.1.1 Environmental Potentials of Nano Technology

According to research communities agenda and some of which as described by Drexler in his books, nanotechnology promises to show major advances in the fields of materials and manufacturing, environmental and energy, electronics and computers, medical and health, and space and aircraft. In research community there are statements that nanotechnology is still not well defined (Maynard, 2007). Some define it on the basis of physical dimension of structures ranging from 0.1 nm to 100 nm; the meaning is different for different disciplines of people, definitions of nanotechnology are as diverse as its applications.

Water purification and desalinization are some of the focus areas of preventive defense and environmental security since they can meet future water demands. Nanotechnology based devices for water desalinization have been designed to desalt sea water, like the use of carbon nanotubes. Carbon nanotubes enhances water purification technologies to the point where they can far out compete reverse osmosis or distillation processes using at least 10 times less energy than reverse osmosis and at least 100 times less energy than

distillation (Ellis, 2004). The other source of water, ground water is traditionally treated through iron treatment walls to reduce the organic and inorganic environmental contaminants, which currently involves granular or “micro-scale” iron (>50,000 nm). The same process under nano technology uses nano-sized iron, which can enhance the reaction, as it is more reactive and effective than macro-scale iron. Its smaller size also makes it more flexible to penetrate (Wenzhon *et al.*, 2008).

ZnO-based materials have size and morphology dependent physical and chemical properties at the nanoscale which could offer tremendous opportunities for advanced technologies. For example, nanostructured ZnO is being actively explored in light emitting diodes, laser diodes, sensors, piezo-electronics, solar cells, UV-blocking components, photo-catalysis, and transparent conductive glass coatings. Various kinds of ZnO nanostructures have been reported ranging from uniform nanobelts, nano-tubes to nano wires. Unique structures could introduce additional tunable properties (Wenzhon *et al.*, 2008).

In the context of semiconductor photo catalysts for water treatment, ZnO nanostructures could offer various advantages. Non-biodegradable dyes widely used in textile, paper and other industrial application pose severe threats to aqueous environments when released without treatment. The elimination of harmful components (including dyes) from wastewater is an important goal for environmental control in industrial settings. Adsorption and chemical coagulation are traditionally used for the treatment of

such wastewater. However, the traditional methods transfer dyes, and the solid waste containing dyes is hard to handle. On the other hand, semiconductor photo-catalysts such as ZnO utilizing photo-induced oxidation process could decompose the dyes effectively. Both powder and thin film forms of ZnO have been explored to date for environmental applications. Powder-form ZnO semiconductor photo-catalysts normally show higher photo-efficiency due to the increased active surface area. However, the powder form photo-catalysts used in suspension state in water have certain limitations due to particle aggregation and technical challenges in photo-catalyst separation and recovery. In comparison, thin film ZnO can be easily recovered, yet its surface area is low leading to poor overall efficiency (Shipra, 2008).

1.2 Problem Statement

Recently quality drinking water has become a major concern worldwide due to the increasing population and decreasing energy resources. Therefore, the efficient treatment of waste waters has become of immediate importance among scientific communities around the globe as there is a growing need to come out with the state-of-the-art technologies that are capable to solve the problems. Ideally an effective waste water treatment is to mineralize completely all the toxic contaminants in waste water without leaving any hazardous residues. In addition the waste water treatment process should be cost effective and feasible for large scale applications.

Water bodies are increasingly choking with wastes ranging from uncollected garbage, industrial wastes inform of heavy metals and synthetic dyes among the many. There are many known sources of heavy metals that find their way to water bodies. The wastes have accumulated in the river sediments and in water to a level which pose precarious effects to human health, aquatic life and the environment. The common polluting heavy metals are lead, calcium, copper, chromium, selenium and mercury.

Large scale production and extensive application of synthetic dyes cause considerable environmental pollution. Dyes are difficult to decompose biologically and chemically. Colour removal in textile and effluents from paper industries remains a serious challenge and the cause of serious effects in water bodies as it reduces light penetration and hence death of aquatic life.

In an effort to reduce the environmental effects of the above (heavy metals and dyes) various techniques have been employed. These techniques include coagulation and sedimentation in which sediments again create disposal problems. Other techniques include the use of constructed wetlands but are expensive to construct, require more space and minimal chances of success as the ecological conditions may not favor particular plant species that are known to remove heavy metals. Nano technology is a promising field in waste water treatment. The aim of this study was to assess the use of synthesized ZnO nanoparticles in photo degradation of dyes and heavy metals adsorption from waste water.

1.3 Justification

Toxic dyes are very important in the view point of environmental protection, because they produce toxic aromatic amines and have other harmful environmental effects. They are widely used and have low degradation rates by aerobic treatment processes. Many of dye molecules are resistant to biological degradation (Baoueret *al.*, 2001). Dying industries use approximately 10,000 dyes and pigments, which are manufactured 7×10^5 tons per year, 50% of them are hazardous (Zhu *et al.*, 2000). Approximately 15% of synthetic toxic are discharged into waste waters.

The existing methods for industrial effluents treatment such as flocculation and sedimentation cause disposal problems, while constructed wetlands for heavy metals removal are expensive. The use of ZnO nanoparticles in photo catalytic colour removal and adsorption of heavy metals is cheaper in cost and does not pose disposal challenge, also the technology uses small amount of energy. The use of nanomaterials like ZnO nanoparticles offers a promising technology for reduction of global environmental pollutants. This semi-conductor catalyst has been preferred because of its wide energy band gap, high photo sensitivity, stability and low cost.

Methyl orange was used as a model dye since it's an organic dye similar to that used in the textile and paper industries. The metal species (Ni^{2+} , Cd^{2+} , and Cu^{2+}) were selected because of their known toxicological effects on humans and high levels of exposure (Gilleret *al.*, 1998).

1.4 Objectives

1.4.1 General Objective

The general objective of this study was to synthesize ZnO nanoparticles and use it as an adsorbent and a photo-catalyst in remediation of waste water.

1.4.2 Specific Objectives

The study was guided by the following specific objectives;

1. To synthesize ZnO nanoparticles by precipitation method
2. To characterize the synthesized ZnO nanoparticles using PXRD, FTIR, SEM and EDX instrumental methods.
3. To determine the extent of removal of Ni, Cd and Cu using ZnO nanoparticles.
4. To determine percentage removal of the methyl orange using ZnO nanoparticles

1.5 Research questions

This research was guided by the following questions

1. Can ZnO nanoparticles be synthesized using precipitation method?
2. What is the size, morphology and distribution of ZnO nanoparticles?
3. What is the extent of removal of Ni, Cu and Cd when treated with ZnO nanoparticles?
4. What is the percentage removal of the methyl orange using ZnO nanoparticles?

CHAPTER TWO

LITERATURE REVIEW

2.1 Synthesis of ZnO nanoparticles

Synthesis of nanoparticles is most commonly done based on three strategies; liquid-phase synthesis, gas-phase synthesis, vapor-phase synthesis. Under liquid phase synthesis the techniques used for synthesis are: precipitation, sol-gel processing, micro-emulsions, hydrothermal/solvo-thermal Synthesis, microwave synthesis, sono-chemical synthesis and template synthesis (Jagadish and Pearton, 2006). The method of synthesis of nanoparticles depends upon the desired physical and chemical properties such as size, size disparity, shape, surface state, crystal structure, organization onto a support, and dispensability. The current study adopted precipitation technique. This involves precipitating zinc oxide using zinc acetate ($\text{Zn}(\text{CH}_3\text{COO})_2 \cdot \text{H}_2\text{O}$) and ammonium carbonate ($\text{NH}_4)_2\text{CO}_3$ (Lanjeet *al.*, 2013).

2.2 Structural Characterization of Nanoparticles

Characterization is the act of describing distinctive characteristics or essential features or qualities of a chemical substance in order to get exact information about the crystal structure, surface morphology, and particle size among others (Dann, 2000). The following characterization techniques are applied; XRD (X-ray diffraction), SEM (scanning electron microscope), transmission electron microscope (TEM), and Fourier

transform infrared spectroscopy (FTIR). In this study, characterization was done using PXRD and FTIR, EDX and SEM.

2.2.1 XRD (X-ray diffraction)

Widely used for precise determination of the position of action in molecules and solids (inorganic) X-rays interact with electrons in matter. When a beam of X-rays impinges on a material it is scattered in various directions by the electron clouds of the atoms. A beam of electrons striking a metal target will eject electrons from energy levels close to the nucleus some of metal atoms. Once vaccines have been created, electrons from higher energy levels fall down into these orbitals; the difference will be emitted as an X-ray of precise energy.

The electrons are created by heating tungsten filaments in a vacuum and then accelerated by a high voltage towards a metal target. Core electrons are knocked out of the metal target and X-rays characteristics of the metal target are produced by decay. Single X-rays must be selected from the tube to carry out the X-ray experiment. Once a single X-ray has been selected, the beam is collimated by passing it through a slit to remove wavelengths other than the desired one before interaction with the sample and finally detection of scattered X-rays (Dann, 2000).

2.2.2 Powder diffraction

A powdered sample contains an enormous number of very small crystals which randomly adopts the whole range of possible orientations. When an X-ray beam strikes a powdered

sample, it is diffracted in all possible directions as governed by Bragg's equation. Each lattice space can give rise to a cone of diffraction. These cones join to form a continuous cone. To analyze the data, the positions of the cones need to be measured using photographic film or by a detector. The actual pattern resulting from a powdered sample is similar to the single crystal experiment in which the data are generated from the particular arrangement of atoms within the unit cell. Factors affecting the intensity of peaks are: lattice type, symmetry, unit cell parameters, distribution and type of atoms in the unit cell. All crystalline solids have a unique powder X-ray diffraction pattern in terms of positions and intensities as the observed reflections (Dann, 2000).

Up to 1895 the study of matter at the atomic level was a difficult task but the discovery of electromagnetic radiation with 1 \AA (10^{-10} m) wavelength, appearing at the region between gamma-rays and ultraviolet, makes it possible. As the atomic distance in matter is comparable with the wavelength of X-rays, the phenomenon of diffraction finds its way through it and gives many promising results related to the crystalline structure. The unit cell and lattices which are distributed in a regular three-dimensional way in space form the base for a diffraction pattern to occur. These lattices form a series of parallel planes with their own specific d-spacing and with different orientations exist. The reflection of incident monochromatic X-ray planes of crystal lattices when the difference between the planes is of a complete number n of wavelengths leads to the famous Bragg's law:

$$n\lambda = 2d \sin\theta \text{ ----- } 1$$

Where n is an integer 1, 2, 3..... λ is wavelength in angstroms (1.54 Å for copper), d is interatomic spacing in angstroms, and θ is the diffraction angle in degrees (Kacheret *al.*, 2009). Figure 2.1 shows Reflection of incident monochromatic X-ray from successive planes of crystal lattices.

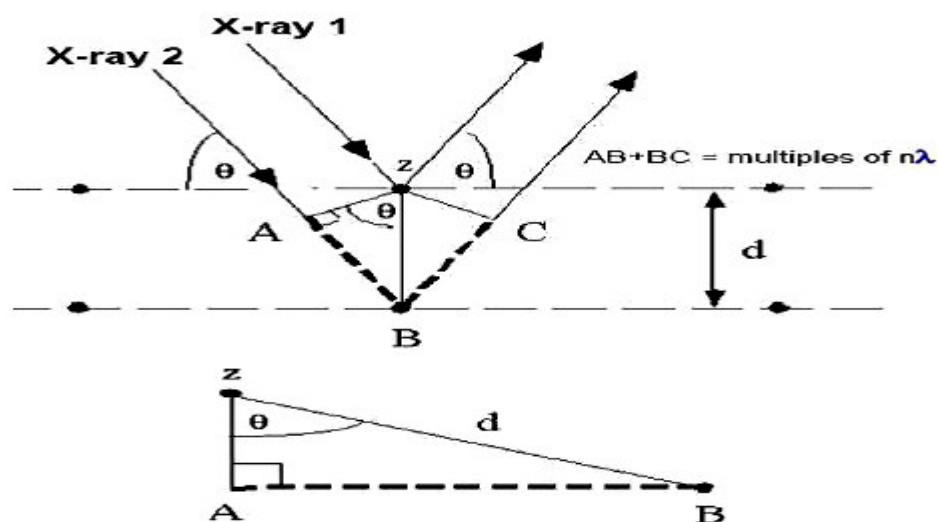


Figure 2.1: Reflection of incident monochromatic X-ray from successive planes of crystal lattices (Source: Authier, 2006)

Plotting the angular positions and intensities of the resultant diffracted peaks of radiation produces a pattern, which is characteristic of the sample. The fingerprint characterization of crystalline materials and the determination of their structure are the two fields where XRD has been mostly used. Unique characteristic X-ray diffraction pattern of each crystalline solid gives the designation of “fingerprint technique” to XRD for its identification. XRD may be used to determine its structure, that is, how the atoms pack

together in the crystalline state and what the inter-atomic distance and angle are to name a few. From these points it can be concluded that X-ray diffraction has become a very important and powerful tool for structural characterization (Özgüret *et al.*, 2005).

2.2.3 Fourier Transform Infrared Spectroscopy (FTIR)

In the region of longer wavelength or low frequency the identification of different types of chemicals is possible by this technique of infrared spectroscopy and the instrument requires for its execution is Fourier transform infrared (FTIR) spectrometer. The spectroscopy merely based on the fact that molecules absorb specific frequencies that are characteristic of their structure termed as resonant frequencies that is the frequency of the absorbed radiation matches the frequency of the bond or group that vibrates. And the detection of energy is done on the basis of shape of the molecular potential energy surfaces, the masses of the atoms, and the associated vibronic coupling. Sometimes the help of approximation techniques like Born–Oppenheimer and harmonic approximations are also taken (Worth & Cederbaum, 2004). As each different material is a unique combination of atoms, no two compounds produce the exact same infrared spectrum. Therefore, infrared spectroscopy can result in a positive identification (qualitative analysis) of every different kind of material. In addition, the size of the peaks in the spectrum is a direct indication of the amount of material present (Howe and Macintosh,

1991). FTIR can be used to analyze a wide range of materials in bulk or thin films, liquids, solids, pastes, powders, fibers, and other forms. FTIR analysis can give not only qualitative (identification) analysis of materials, but with relevant standards, can be used for quantitative (amount) analysis. FTIR can be used to analyze samples up to ~11 millimeters in diameter, and either measure in bulk or the top ~1 micrometer layer. FTIR spectra of pure compounds are generally so unique that they are like a molecular "fingerprint" (Flemming *et al.*, 1991).

2.2.4 Energy dispersive X-ray Spectroscopy (EDX)

EDX makes use of the X-ray spectrum emitted by a solid sample bombarded with a focused beam of electrons to obtain a localized chemical analysis. All elements from atomic number 4 (Be) to 92 (U) can be detected in principle, though not all instruments are equipped for 'light' elements ($Z < 10$). Qualitative analysis involves the identification of the lines in the spectrum and is fairly straightforward owing to the simplicity of X-ray spectra. Quantitative analysis (determination of the concentrations of the elements present) entails measuring line intensities for each element in the sample and for the same elements in calibration standards of known composition (Goldstein, 2003).

By scanning the beam in a television-like raster and displaying the intensity of a selected X-ray line, element distribution images or 'maps' can be produced. Also, images produced by electrons collected from the sample reveal surface topography or mean atomic number differences according to the mode selected.

The EDX spectrum is displayed in digitized form with the x-axis representing X-ray energy (usually in channels 10 or 20 eV wide) and the y-axis representing the number of counts per channel. An X-ray line (consisting of effectively mono-energetic photons) is broadened by the response of the system, producing a Gaussian profile. Energy resolution is defined as the full width of the peak at half maximum height (FWHM). Conventionally, this is specified for the Mn K α peak at 5.89 keV. For Si(Li) and SDD detectors, values of 130-150 eV are typical (Ge detectors can achieve 115 eV). The resolution of an EDX is about an order of magnitude worse than that of a WDS, but is good enough to separate the K lines of neighboring elements (Scott and Love, 1994).

The object of qualitative analysis is to find what elements are present in an 'unknown' specimen by identifying the lines in the X-ray spectrum using tables of energies or wavelengths. Ambiguities are rare and can invariably be resolved by taking into account additional lines as well as the main one. The ED spectrometer is especially useful for qualitative analysis because a complete spectrum can be obtained very quickly. Aids to identification are provided, such as facilities for superimposing the positions of the lines of a given element for comparison with the recorded spectrum (Scott and Love, 1994).

2.2.5 Scanning Electron Microscope (SEM)

A scanning electron microscope (SEM) is a type of electron microscope that produces images of a sample by scanning it with a focused beam of electrons. The electrons interact with atoms in the sample, producing various signals that can be detected and that

contain information about the sample's surface topography and composition (Soltaninezhad and Amrnifar, 2011). The electron beam is generally scanned in a raster scan pattern, and the beam's position is combined with the detected signal to produce an image. SEM can achieve resolution better than 1 nanometer. Specimens can be observed in high vacuum, in low vacuum, in wet conditions (in environmental SEM), and at a wide range of cryogenic or elevated temperatures (Joshi and Shrivastava, 2012).

The most common mode of detection is by secondary electrons emitted by atoms excited by the electron beam. On a flat surface, the plume of secondary electrons is mostly contained by the sample, but on a tilted surface, the plume is partially exposed and more electrons are emitted. By scanning the sample and detecting the secondary electrons, an image displaying the topography of the surface is created (Lynch and Dawson, 2008).

2.3 Nano-Materials and their Environmental Applications

In 1864, James Clerk Maxwell was the first to mention some of the nano-concepts in nanotechnology through a proposed experiment on a tiny entity known as Maxwell's Demon able to handle individual molecules. In the early 20th century, the first observations and size measurements of nano-particles using an ultra-microscope were made possible in a study of gold sols and other nano-materials with sizes down to 10 nm and less (Zsigmondy, 1914). Zsigmondy was the first to characterize particle sizes using the term nanometer and he developed the first system of classification based on particle size in the nanometer range. Several advances in the field of nanomaterial

characterization were possible with Langmuir in 1920s introduced the monolayer concept, and Derjaguin in 1950s conducted the first measurement of surface forces (Derjaguin, 1954). Feynman (1959) at an American Physical Society meeting at Caltech described a proposed process to manipulate individual atoms and molecules by using one set of precise tools (Gribbin, 1997).

Since then, several advances were made in the study of nanoscale structures, but the term nanotechnology was first defined by Taniguchi (1974) as "nanotechnology mainly consists of the processing of, separation, consolidation, and deformation of materials by one atom or one molecule". The tools and methods for nanotechnology involve imaging, measuring, modeling, and manipulating matter at the nano-scale. In 1980s, nanotechnology and nanoscience got a boost with two major developments: the birth of cluster science and the invention of the Scanning Tunneling Microscope (STM). Major current tools for nanotechnology measuring include many devices such as STM, Scanning Probe Microscopes (SPMs), Atomic Force Microscopy (AFM) and Molecular Beam Epitaxy (MBE) (Roco, 1999).

Diagnosis of particles at the nano-scale level contributed extensively to the production, modification and shaping of structures that were used in different industrial, health and environmental application. Nanostructure science and technology is a broad research area that encompasses the creation of new materials and devices from nanosized building blocks (Hu and Shaw, 1998). Building blocks are used to make molecules that are arranged in nanostructures and nanomaterials with dimensions of 1 to 100 nm. This

process is known as a "bottom up" approach where building blocks are arranged and then assembled to form larger size materials. The formation of powder components (structural composite material) through aerosol techniques is a main example of this approach (Wu *et al.*, 1993). Many other approaches are being used to synthesize and assemble nanostructures but the critical point remains in the control of the size and composition of nanocluster components and in the control of interfaces and the distribution of nano-components within the fully formed materials (Hu and Shaw, 1998).

Many potential benefits of nanotechnology have already been identified by many researchers in the environmental and water sector, medicine, and in several industrial applications but the future nanotechnology might bring innovations that can answer many existing scientific questions (Fleischer and Grunwald, 2008). Hence, nanotechnology is going to play an important role in addressing fundamental issues on health, energy and water (Binks, 2007).

Major potential environmental benefits of nanotechnology were reported in the draft nano-materials research strategy by (Savage and Wentzel, 2008), including: early environmental treatment and remediation, stronger and lighter nano materials, smaller, more accurate and more sensitive sensing and monitoring devices. Additional benefits lay in the cost-effective use of renewable energy, low energy requirement and low waste generation devices, early disease detectors for preventive treatment, pollution control, and the prevention and remediation using improved systems. For the purpose of

improving the above listed treatment processes, the use of nano-materials is being researched to fabricate separation and reactive media which is of high quality in terms of reactivity and performance (Bellona and Drewes, 2007).

Additionally, the use of nano-materials and nanoparticles to bio-remediate and disinfect wastewater is gaining popularity (Mohan and Pittman, 2007). For instance, metal oxide nano-materials such as TiO_2 are among the promising nano-catalysts that were tested successfully for their antimicrobial activity. Moreover, fullerenes (C_{60}) as pollution tracers are being used to provide contaminant-fate information to assist in developing water remediation strategies. Magnetic nanoparticles are being developed to adsorb metals and organic compounds; and nano-catalysts are being explored to reduce pollution of oxidized contaminants (Hillie and Munasinghe, 2006). Metal processing wastewater often contains hexavalent chromium species, Cr (VI), which are toxic and can act as carcinogens, mutagens and teratogens in biological systems (Dupont and Guillon, 2003).

Metal industries are required to reduce the amount of chromium in their effluent to around 0.1 mg/L (Ayuso *et al.*, 2003) before discharging it into the sewer system. Maghemite nanoparticles were studied for their potential in removing and recovering chromium from wastewater. Hu *et al.* (2005) developed a new method by combining the adsorption ability of nanoparticles and the magnetic separation technique. The method was space-saving, cost-effective, simple, and environmental-friendly. Additionally, chromium was successfully removed from the wastewater and the nano-scale maghemite

retained the original metal removing capacity after six adsorption-desorption cycles. The adsorption was pH dependent with optimal adsorption at pH 2.5.

2.4 Application of Nanotechnology in Water and Wastewater Treatment

Nanotechnology is being applied in the production of water purification membranes. Recently, Theron *et al.* (2008) reported the following water filtration membranes produced from nano-materials: nanostructured membranes from nano-materials such as carbon nanotubes, nanoparticles and nano-reactive membranes from metal nanoparticles and other nano-materials. On the other hand, adsorption is considered as an effective, efficient and economic method to remove water contaminants (Jiuhui, 2008). Effective adsorbents include: activated carbon, clay minerals and silicas, zeolites, metal oxides, and modified composites (Zhang *et al.*, 2005). The decomposition of organic compounds in water as well as the disinfection of water under UV light using TiO₂ mediated photo-catalyst is gaining popularity as the effectiveness of the photo-catalysts has been demonstrated by many scientific studies (Kumar *et al.*, 2008).

Nanotechnology for water remediation will play a crucial role in water security and consequently the food security of the world. The applications of nanotechnology in the cleanup of contaminated water could be summarized (Smith, 2006): nano-scale filtration techniques, adsorption of pollutants on nanoparticles and breakdown of contaminants by nanoparticle catalysts.

2.5 Photo-catalytic Degradation of Dyes

Paper, dyeing, plastic, and textile industries use colour for dyeing their products and thus use a huge amount of water, which results in the production of a dye-containing wastewater with hazardous effects on the environment (Sreedhar and Kotaiha, 2006). At present, 100,000 different types of dyes with annual production rate of 7.0×10^5 ton, are produced. Among them textile industries consume about 36,000 ton/year dye, 10 to 20 percent of which remains in wastewater (Gregorio, 2006). Degradation of organic materials existing in the environment which occurs according to the above process with radiation of ultraviolet light on the surface of zinc oxide is called photo-catalytic reaction of ZnO (Vijay *et al.*, 2009). Basis of ZnO/UV photo-catalytic process is the semi-conduct optical stimulation of ZnO as a result of electromagnetic ray absorption. ZnO has an energy band of 3.2 eV which can be activated by radiation of UV in the wavelength of 387.5 nm. On the earth's surface, sunlight begins in the wavelength of 300 nm and only 4-5 percent of solar radiation may be used by ZnO.

Surface area and number of active places used by the catalyst for absorbing pollutants, play an important role in degradation level, among known catalysts like ZrO_2 , ZnO and TiO_2 . High efficiency of ZnO has been approved and confirmed in many studies, ZnO is not poisonous and has high stability and very good performance and is also cheaper (Awitor *et al.*, 2008). An advantage of photo-catalytic method includes low temperature, low expenses and also radically low level of energy consumption in this method. These

factors have caused the photo-catalysts to be used in commercial scales.(Rajeswari and Kanmani, 2009).A significantly great number of researches and articles have been published regarding removal of dangerous and poisonous compounds from water, wastewater and air, using photo-catalytic methods (Zhang *et al.*, 2010).

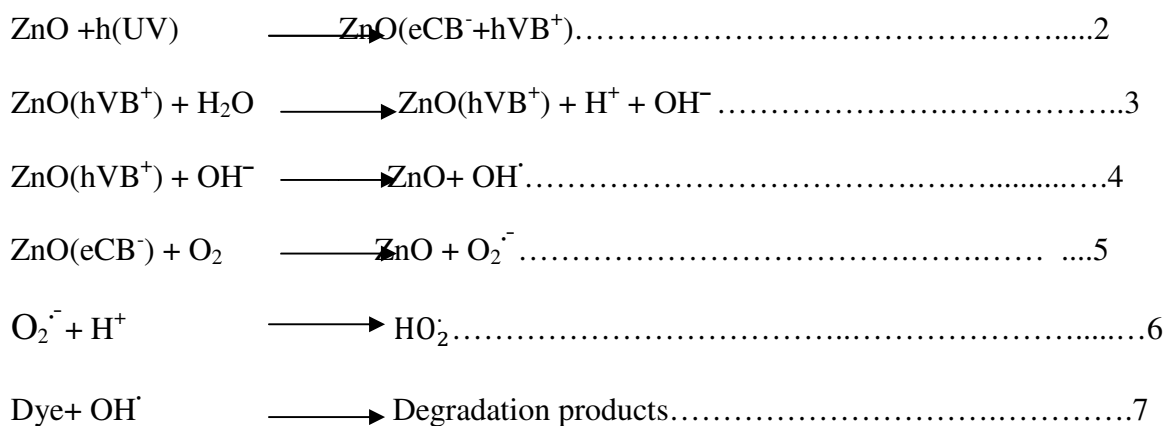
2.6Dye Photo-catalytic degradation Mechanism

Advanced oxidation processes (AOPs) are alternative techniques of destruction of dyes and many other organic in waste water and effluents. These processes generally involve UV/H₂O or UV/O₃ for the oxidative degradation of contaminants. Semiconductor photocatalysis is a newly developed AOP which can be conveniently applied to dye pollutants for their degradation. AOPs produce OH[•]Radicals which are powerful oxidizing agents and completely degrade most organic pollutants.Photocatalytic process is the semiconductor optical stimulation of ZnO as a result of electromagnetic ray absorption. ZnO has an energy band of 3.2 eV which can be activated by radiation of inUV wavelength of 387.5nm (Daneshvaret *al.*, 2004).

On the earth's surface, sunlight begins in the wavelength of 300nm and only 4 – 5% of solar radiation may be used by ZnO. Surface area and number of active sites used by the catalyst for absorbing pollutants plays an important role in degradation level (Awitor *et al.*, 2008). Upon irradiation valence band electrons are promoted to the conduction band leavingholes behind. These electron hole pairs caneither recombineor can interact separately with other molecules. The holes may react either with electron donors in the

solution or with hydroxide ions to produce powerful oxidizing agents like OH^\cdot (Oxidation potential 2.8V) or superoxide radicals (O_2^\cdot) (Tang and Huren, 1995).

Nanosized ZnO semiconductor acts as a sensitizer for light – induced redox processes due to the electronic structure of the metal atoms in chemical combination which is characterized by a filled valence band and an empty conduction band (Hoffman, 1995). The relevant reactions at the semiconductor surface causing degradation of dyes can be expressed as;-



The resulting OH^\cdot radical, being a very strong oxidizing agent (standard redox potential +2.8 V) can oxidize most of methyl orange dye particles (Hoffman, 1995). The scheme below illustrates photo degradation process.

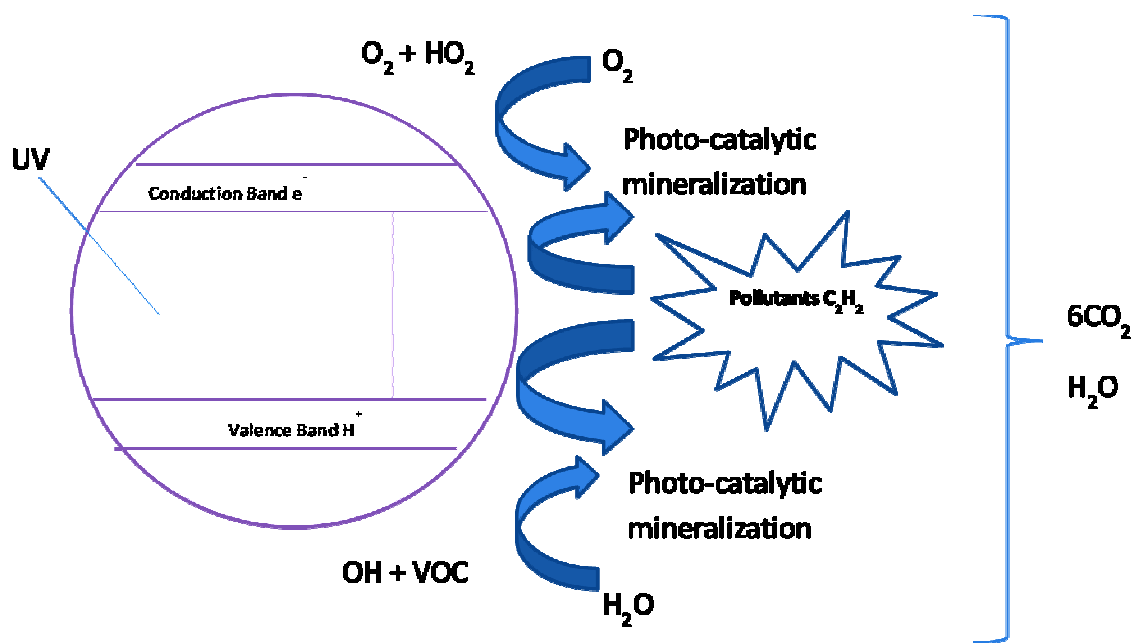


Figure 2.2: Summary of photo-catalytic degradation of dyes (Sampa and Biney, 2004)

The quantum efficiency of ZnO powder is significantly larger than other semiconductors and higher catalytic efficiencies have also been reported. The biggest advantage of ZnO is that it absorbs over a larger fraction of solar spectrum and for this reason, ZnO photo catalyst is the most suitable for photocatalytic degradation in presence of sunlight (Sampa and Biney, 2004).

2.7 Health Effects of heavy metals

According to the WHO (2006) the limit of the toxicity value for nickel is 130 μgL^{-1} , assuming a 60 kg adult drinking two litres of water per day. However, the presence of nickel at higher levels in the human body can cause serious lung and kidney problems as well as gastrointestinal distress, pulmonary fibrosis and skin dermatitis. A further

neurotoxin is mercury, which can cause damage to the central nervous system, and its concentration within the range of $0.12\text{--}4.83\text{ mgL}^{-1}$ may cause the impairment of pulmonary and kidney function, chest pain and dyspnea (Authier, 2006).

As per the USEPA(2005), cadmium is a plausible human carcinogen, and its presence potentially damages human physiology and other biological systems when the tolerance levels are exceeded. High levels of cadmium exposure (1 mgm^{-3}) may result in several complications leading to death.

Manahan (2000) described Cd to be very similar to zinc, and may replace zinc in some enzymes, thereby altering stereo-structure and impairing its catalytic activity. Duffus (2002) stated that, in small doses Cd causes vomiting, diarrhea, and colitis. Continuous exposure to Cd causes hypertension, enlargement of heart, and premature death. There is evidence that, Cd causes chromosomal abnormalities and may exert carcinogenic effects on lungs.

WHO (2006) indicates that, acute Cu poisoning in humans is very rare, and it usually results from contamination of food stuff or beverages by Cu containers or from accidental ingestion of gram quantities of Cu salt, symptoms of acute Cu poisoning include; salivation, epigastric pains, nausea, vomiting, and diarrhea all of which are probably due to irritant effect of Cu on the Gastro- intestinal mucosa.

Cd and Ni are widely dispersed in the environment, these elements have no beneficial effects in humans, and there is no known homeostasis mechanism for them (Vieira *et al.*,

2011). They are generally considered the most toxic to humans and animals; the adverse human health effects associated with exposure to them, even at low concentrations, are diverse and include; neurotoxic and carcinogenic actions (Tokar *et al.*, 2011).

2.8 The use of metal oxides nanoparticle as heavy metals adsorbent in waste water

Nanoparticles have two key properties that make them particularly attractive as sorbents. On a mass basis, they have much larger surface areas than bulk particles. Nanoparticles can also be functionalized with various chemical groups to increase their affinity towards target compounds. It has been found that the unique property of nanoparticles is to develop high capacity and selective sorbents for metal ions and anions. Photo-catalytic nanomaterials allow ultraviolet light also used to destroy pesticides, industrial solvents and germs (Yantasee *et al.*, 2007).

Zinc oxide nanoparticles have been used to remove arsenic from water, even though bulk zinc oxide cannot absorb arsenic. Some adsorption processes for wastewater treatment have utilized ferrites and a variety of iron containing minerals, such as akaganeite, ferrihydroxide, ferrihydrite, goethite, hematite, lepidocrocite, magnetite and maghemite. Adsorption of organics to the nanoparticle media was extremely rapid (Apiratikul and Pavasan, 2008).

More than 90% of the organics is adsorbed within 30 minutes. The isotherm studies indicated that, on a surface area basis, the adsorption capacities of the nanoparticle media were significantly (>2 folds) higher than the ferric oxide media typically used in water

treatment (Pitcheret *et al.*, 2004). The smaller size of magnetic nanoparticles, which are 2-3 orders of magnitude smaller than a bacterium, provides extra benefits compared to magnetic beads. When their surface is appropriately elaborated, magnetic nanoparticles can also provide efficient binding to the bacteria because their high surface/volume ratio simply offers more contact area.

Iron (Fe) nanoparticles, nanodots or nanopowder are spherical or faceted high surface area metal nanostructure particles. Nanoscale iron particles are typically 20-40 nanometers (nm) with specific surface area (SSA) in the 30-50 m² g⁻¹ range (Bhattacharyya and Gupta, 2008).

The use of iron ferrite and magnetite in wastewater treatment has a number of advantages over conventional flocculent precipitation techniques for metal ion removal. The high surface area to mass ratios of nanoparticles can greatly enhance the adsorption capacities of sorbent materials. In addition to having high specific surface areas, nanoparticles also have unique adsorption properties due to different distributions of reactive surface sites and disordered surface regions (Wuet *et al.*, 2009).

2.9 Adsorption mechanism

In order to understand the mechanism of the adsorption of metal ions by nanoparticles, a number of efforts have been undertaken in investigating the influence of the adsorption process using different techniques, such as infrared (IR) spectroscopy, X-ray diffraction (XRD), X-ray photoelectron spectroscopy (XPS) and extended

X-ray absorption fine structure (EXAFS) spectroscopy. The basis of discussion includes physical adsorption, surface complexation, ion exchange, electrostatic interaction and hard/soft acid-base interaction. In general, the negatively-surface-charged nanoparticles form a complex with metal ions above their point (Singh, *et al.*, 2011).

The enhanced complex tendency of adsorbent at higher pH is expected, as at lower pH the active sites are occupied with H^+ and are released at a higher pH, thereby originating the desired complex formation. Also, at lower pH, H^+ ions are adsorbed onto the surface of nanoparticles, leading to a net positive charge. A certain amount of metal ions can still be adsorbed by nanoparticles at $pH < pH_{pzc}$. This is perhaps due to the fact that ion exchange takes place at $pH < pH_{pzc}$. Since the affinity of metal ions to nano ZnO is higher than that of H^+ ions, metal ions can replace the adsorbed H^+ ions from the ZnO surface by an ion exchange mechanism. The adsorption of metal ions by ion exchange is relatively slow when compared to surface complexation, since the organic molecules present on the surface of the nanoparticles may cause steric hindrance towards the adsorption of metal ions (Kansalet *et al.*, 2006).

2.10 Toxicological Effects of Nano Materials

Knowledge of the potential toxicity of nanoparticles is limited but growing rapidly. Most of the work that has been done so far addresses primarily the occupational hazards associated with the manufacture and handling of nanostructured materials. There is a body of review papers available (Lynch and Dawson, 2008) that suggest that, owing to

their increased specific surface area and potentially altered bio-kinetics, nanoparticles may have a toxicity profile that deviates from that of their bulk equivalents. The toxicity of the nanomaterial, however, may be less than, greater than or similar to that of the bulk material, depending on the characteristics both of the material of which it is composed and of the particle itself (USEPA, 2005).

The relationship between the nanomaterial and the bulk material may depend on the dose metrics used in the comparison. There are only a limited number of published oral toxicity studies on some classes of nanomaterials, with those on solid particulates largely limited to insoluble metals and metal oxides. The quality of many of these studies is questionable, severely limiting the use of this information for risk assessment purposes. Common limitations include: use of a single size of nanomaterials, poor characterization and its administration at unrealistically high doses, study of only a narrow range of biological parameters, or omission of an appropriate larger particle of the same composition and a soluble form of the parent material as comparators to allow distinction between the effects of particle sizes and those of release of particle surface material into solution (Oberdorster *et al.*, 2007). This leads to the conclusion that the current state of knowledge does not permit reliable prediction of the toxicological characteristics of any given nanomaterials.

The capacity to predict computationally (such as using Quantitative Structure–Activity Relationship (QSAR)) the toxicological properties of conventional materials, however,

although considerably greater than for nanomaterials, is nonetheless limited and of variable reliability. It does not only trigger biological effects, but may adsorb or bind proteins or other compounds on their surfaces (Lynch and Dawson, 2008). This selective binding and carrier potential has been termed a “Trojan horse” effect. The use of a nano-carrier to increase the bioavailability of bioactive compounds raises similar issues. The suggestion is that these carrier systems might impact the absorption of molecules, for example by introducing unintended molecules such as undigested or un-metabolized compounds across the gastro intestinal tract, leading to unintended effects. For example, chitosan can adsorb fat, including fat soluble micronutrients, and thereby prevent their absorption in the gastro intestinal tract. These issues, and the potential to disrupt the gastro intestinal barrier, will need to be addressed during the safety assessment of nanomaterials that have this potential, and in particular will require a careful consideration of the bio-kinetics and binding characteristics of the nanomaterials under consideration (USEPA, 2005).

2.11 Stabilizing agents

Most organic stabilizers for semiconductor nanoparticles used such as organic thiols, oleic acids, urea, oxalic acids and others are water soluble. ZnO nanoparticles give significant stability under any type of stabilizer (Herrmann and Helmoltz, 2010). Oxalic acid is an organic compound which is used during synthesis of ZnO nanoparticles. It is used as a chemical capping in which it is used to passivate the surface of particles so that they

do not agglomerate or ripen to form larger particles. This ensures that the nanoparticles synthesized yields stable product with uniform size distribution (Zaidi and Pant, 2008).

The capping agent provides protective organic shell to particles to prevent the nanoparticles from aggregating in solution. It also promotes formation of fewer, larger nuclei and thus nanocrystal particle sizes (Gnanasangeetha and Sarala, 2013). Stabilizers enable the nanoparticles to be resistant to deactivation and thus its performance which depends on the nature and concentration of the stabilizing agent used. The difference in performance is due to electrical conductivity of stabilizers, the morphology and interface roughness and stabilizer particle interaction (Hu *et al.*, 2003).

The crystal structure of nano ZnO without as well as with oxalic acid has no effect on ZnO's wurzite structure as revealed by X-ray diffraction. SEM reveals different nature of surfaces and microstructures for nano ZnO obtained with and without stabilizers (Rajesh and Raychaudhuri, 2013).

2.12 Related studies

Shanthi and Muthuselvi (2012) studied morphology of synthesized nano ZnO using PXRD, FTIR and SEM. The PXRD results indicated particle size of 12nm, 16nm and 18nm for the three samples, all of which fall within the nano scale range of below 100 nm. Rashed and El-Amin (2007) conducted a study on photo catalytic degradation of methyl orange in aqueous ZnO nanoparticles under different solar radiation sources. The results

revealed that; the degradation rate increases with the increase of dye concentration to a certain concentration, and further increase leads to a decrease in dye degradation rate.

The FTIR analysis showed a broad band between 430-419 cm^{-1} . The spectra showed bands at 3250 and 3500 cm^{-1} which they assigned to OH stretching vibrations of adsorbed water or residual Zn(OH)_2 present in the bond. The images obtained from SEM for the samples showed sphere and cube like nanoparticles distributed well within the range of ~ 100 nm. On the effects of irradiation sources; the study revealed that decolourization efficiency of 98.92% was observed at 90 minutes irradiation time under solar light whereas in presence of UV radiation, for the same duration, only 50% decolourization efficiency was recorded (Rashed and El-Amin, 2007).

Singh *et al.* (2011) reported on the removal of various toxic metal ions, such as Co^{2+} , Ni^{2+} , Cu^{2+} , Cd^{2+} , Pb^{2+} , Hg^{2+} and As^{3+} from wastewater by ZnO nano-particles. It was reported that Hg^{2+} , Pb^{2+} and As^{3+} have a stronger attraction towards ZnO nano-particles due to their high electro-negativity and, hence, that they exhibit better removal efficiency (63.5% Hg^{2+} , 100% Pb^{2+} and 100% As^{3+}).

Kumar *et al.* (2013) demonstrated the removal of Pb(II) and Cd(II) under different adsorbate concentrations, contact times, adsorbent dosages, pH and temperature conditions, from aqueous solutions using ZnO nano-particles. They observed the maximum adsorption capacities of Pb(II) and Cd(II) to be 160.7 and 147.25 mg per g, respectively. Sheela *et al.* (2012) used ZnO nanoparticles of size 25 nm for the removal

of Cd(II) and Hg(II) ions from an aqueous solution. They found a maximum adsorption capacity of 387 and 714 mg per g for Cd(II) and Hg(II) ions, respectively.

Zinc oxide has received a great deal of attention in relation to the photo catalytic degradation of organic contaminants. It has been reported that different morphologies of ZnO exhibit different degrees of photo catalytic activity. Ma *et al.* (2011) and Zhai *et al.* (2012) have reported on the photo catalytic activity of ZnO nano-particles in decomposing methyl orange (MO) in water under UV irradiation, they noted high catalytic efficiency.

2.13 Adsorption Isotherms for the photocatalytic degradation of dye

Photocatalytic degradation of dye is commonly expressed using two major adsorption isotherms: Langmuir and Freundlich (Romanchuk *et al.*, 2013).

Langmuir adsorption isotherm is the most commonly used due to its simplicity and its ability to fit a variety of adsorption data. It is based on four assumptions:

1. All of the adsorption sites are equivalent and each site can only accommodate one molecule.
2. The surface is energetically homogeneous and adsorbed molecules do not interact.
3. There are no phase transitions.
4. At the maximum adsorption, only a monolayer is formed. Adsorption only occurs on localized sites on the surface, not with other adsorbates.

These four assumptions are seldom all true: there are always imperfections on the surface, adsorbed molecules are not necessarily inert, and the mechanism is clearly not the same for the very first molecules to adsorb to a surface as for the last (Kyzas, Lazaridis & Bikiaris, 2013). The fourth condition is the most troublesome, as frequently more molecules will adsorb to the monolayer; this problem is addressed by the Brunauer–Emmett–Teller (BET) isotherm for relatively flat (non-microporous) surfaces. The Langmuir isotherm is nonetheless the first choice for most models of adsorption, and has many applications in surface kinetics and thermodynamics (Senthamarai *et al.*, 2013).

The theory can be represented by the following equation:

$$\frac{C_e}{Q_e} = \frac{1}{b} Q_0 + \frac{C_e}{Q_0} \text{-----}8$$

Where q_e is the amount of methyl orange adsorbed per unit mass of adsorbent (mg/g^{-1}) and C_e is the equilibrium concentration of methyl orange, Q_0 and b are Langmuir constant related to the capacity and energy of adsorption, respectively.

The Freundlich isotherm is not commonly used. The empirical Freundlich isotherm equation is:

$$Q_e = K \times C_e^{(1/n)} \text{.....}9$$

in logarithmic form (linear)

$$\log Q_e = \log K \times \frac{1}{n} \log C_e \text{.....}10$$

where k is related to adsorption capacity, and n is related to intensity of adsorption.

CHAPTER THREE

MATERIALS AND METHODS

3.1 Research approach

This project achieved its scientific objectives through laboratory experiments that allowed precisely controlled processes. Although laboratory based, the overall research plan was designed to ensure that the results will be used to achieve the project objectives. Experiments were conducted using methyl orange which was used as a model dye. Its mode of removal is similar to synthetic dyes. Stock solutions of Cd^{2+} , Cu^{2+} and Ni^{2+} were prepared and analysis was done using AAS (AA-7000). The experimental plan was carefully constructed to ensure that each objective was addressed by procedures and experiments that yielded the desired outcomes.

3.2 Materials and Reagents

Methyl orange dye (ACS reagent, Dye content, 85%) was obtained from Indo lab chemicals in Eldoret while ZnSO_4 (0.1 M, 99% Purity) and NaOH (0.1 M, 99% Purity) were purchased from Rimoi chemicals, Eldoret. All the reagents were prepared using double distilled water and in glass apparatus. All the materials required for synthesis, adsorption and photo degradation studies was obtained at University of Eldoret.

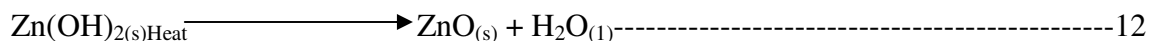
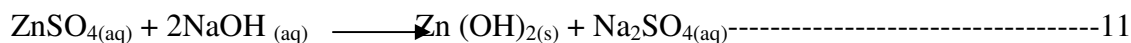
3.3 Synthesis of ZnO nanoparticles

ZnO nanoparticles were synthesized using precipitation method. In this method, ZnO nanoparticles were prepared in two ways. In the first set, 100ml of 1M ZnSO₄ solution was added to 100ml of 2M NaOH solution in drops. When the addition was complete, the mixture was kept at room temperature under constant stirring using magnetic stirrer for a period of 2-4 hours.

The constant stirring using magnetic stirrer makes the precipitation homogeneous and minimal particles which reduce the specific surface free energy of crystal nucleus which inhibit agglomeration and growth of the crystal nucleus so the particle size of the product is reduced (Zhanget *al.*, 2010).

The resultant precipitate obtained was filtered using a filter paper then rinsed with distilled water. The formed white precipitate of Zn(OH)₂ was allowed to settle, filtered using filter paper of pore size 0.4µm in a suction pump, washed with distilled water several times and dried in hot oven at 150⁰C for 45 minutes. The synthesized ZnO nanoparticles were further irradiated at 180 W with microwave radiation in a microwave oven for 30 minutes. This was named as sample L₁. The above procedure was followed to synthesize ZnO nanoparticles in different experimental conditions. ZnSO₄, NaOH and oxalic acid were used as stabilizing agent. Thus one more sample was obtained and referred to as L₂.

The precipitation reaction was represented as



The resultant ZnO nanoparticles particles after irradiation were collected and stored in brown bottles.

3.4 Characterization of ZnO nanoparticles particles

The synthesized ZnO nanoparticles were subjected to (PXRD), (FTIR), at ICRAF Nairobi, (SEM) and (EDX), at The University of western Cape (South Africa) in order to confirm the nanostructure.

3.5 Heavy metal analysis

Atomic absorption spectrometer (AAS) was used to analyze samples for levels of heavy metal species; Cd^{2+} , Cu^{2+} and Ni^{2+} before and after treatment with ZnO nanoparticles. During analysis, the following parameters were varied; heavy metals concentrations, dose of the adsorbent and the pH of solutions.

3.5.1 Optimizing operating conditions

The instrument's operating conditions were optimized before the actual analysis. The fixed parameters were automatically set upon selection of the element to be analyzed. These parameters included; wavelength, lamp current, slit width and extra heat tension (EHT) (Table 3.1). The other parameters were set according to the manufacturers

specifications in the manual (Fang, 1995). The acetylene and oxygen flow rate was set to attain maximum transparency of the flame. The optimized conditions for the AAS instrument during analysis are shown in table 3.1 below.

Table 3.1: Optimized conditions for AAS

Element	Wavelength λ (nm)	Lamp Current (mA)	Slit Width (nm)	Acetylene flow rate (L/min)	Oxidant flow rate (L/min)	BH (mm)	EHT (v)
Cu	324.8	4	0.5	2	13.5	13.5	494
Cd	228.8	4	0.5	2	13.5	13.5	562
Ni	352.4	4	0.5	2	13.5	13.5	582

Key: BH - Burner height, EHT - Extra Heat Tension

(Source: Manahan, 2000)

3.5.2 Calibration Curves

Sensitivity and detection limit checks were carried out to ensure that they were in agreement with the operating parameters by running the stock solution before the actual analysis. Calibration curve for each element were prepared using the standard working solutions. The curves had absorbance in the y – axis and concentrations in the x – axis. This plot was used as standard graph for estimation of metal ion concentration by interpolation technique.

3.5.3 Laboratory-based heavy metals analysis

The concentrations of the adsorbed metals were analyzed using Spectra AA-200 Atomic Absorption Spectrophotometer. A reagent blank sample was taken through the method, analyzed and subtracted from the samples to correct for reagent impurities and other

sources of errors from the environment. The concentrations of the metals were determined in triplicates to ensure accuracy and precision of the analytical procedure.

After adsorption, the concentration of these metal ions was analyzed. The extent of removal in terms of percentage was calculated using the following relationship.

$$\% \text{ Removal} = \frac{C_1 - C_2}{C_1} \times 100 \text{ -----13}$$

Where C_1 = Initial concentration

C_2 = Final concentration

The effect of various experimental parameters on adsorption of heavy metals in the aqueous suspension by ZnO nanoparticles were studied by varying the experimental conditions; concentration of the heavy metals, amount of the sample (L_1 and L_2) and pH.

3.6 Photo-catalytic degradation studies

3.6.1 Preparation of dye solution

Methyl orange (MeO) is an organic dye with a chemical formula of $C_{14}H_{14}N_3SO_3Na$ and characterized by sulphonic groups, which are responsible for high solubility of these dyes in water. The stock solution (1,000ppm) was prepared and stored in brown bottles. The stock solution was diluted to get different required initial concentrations of the dye used. Dye concentration was determined by using absorbance measured before and after the treatment using UV-VIS spectrometer.

3.6.2 Measurement of concentration of dye solution

The stock solution was diluted to different initial concentrations 10, 20, 30, 40 and 50 ppm for methyl orange in standard measuring flasks by making necessary dilutions with required volume of distilled water. The optical density of each dye solution was measured using UV-VIS spectro photometer (model – No-SL-150 Elico) at maximum wavelength value for MeO dye. A plot of optical density versus initial concentration was drawn. This plot was used as standard graph for estimation of dye by interpolation technique. The values of optical density for dye solutions before and after removal of dye were obtained by using UV-VIS spectrophotometer. Using these optical densities the corresponding dye concentration was obtained from the graph.

3.6.3 Determination of extent of removal of the dye

Stock solution of MeO dye (1,000ppm) was suitably diluted to get the required initial concentration from 15 – 45ppm. A 10ml of the dye solution of known initial concentration (C_1) was transferred to 50ml beaker. Required amount of the photo-catalyst (L_1 and L_2) was exactly weighed and then transferred to the dye solution with different C_1 . The beaker was then exposed to fluorescent light and direct sunlight for a fixed period of contact time.

After bleaching, the optical density (OD) of these solutions was measured using UV-Vis spectrophotometer and the final concentrations (C_2) obtained from the standard graph.

The extent of removal of the dye in terms of percentage removal was calculated using the following relationship.

$$\text{Percentage removal} = \frac{100(C_1 - C_2)}{C_1} \text{-----14}$$

Where

C_1 = initial concentration of dye (ppm)

C_2 = final concentration of dye (ppm)

3.7 Factors that govern degradation process

The effect of various experimental parameters on degradation of MeO dye in the aqueous suspension by ZnO nanoparticles were studied by varying the experimental conditions; concentration of the dye, amount of the sample (L_1 and L_2) and contact time. Each test was done in triplicate to ensure accuracy and repeatability.

3.7.1 Effect of variation of initial concentration of MeO dye

Keeping all other factors constant, the concentration of the dye was changed from 15ppm to 45 ppm then exposed to sunlight and fluorescent light energy and its effect on the rate of bleaching was studied.

3.7.2 Effect of variation of dose of photo catalyst on photo degradation of MeO

The initial concentration of the dyes pH and contact time in all beakers were kept constant and the dose of photo-catalyst was varied from 0 mgL^{-1} to 400 mgL^{-1} . The removal of the

dye at optimum initial concentration, 3hrs contact time and pH (6.8) was carried out following the general procedure.

3.7.3 Effect of variation of contact time on the photo-degradation of MeO

In order to study the effect of variation of contact time on the removal of MeO dye by exposure to sunlight and fluorescent light, experiments were carried out with optimum initial concentration of dye solution, pH (6.8) and optimum dose of photo-catalyst in the beakers containing required optimum initial concentration and pH was recorded. Then the optimum dose of photo-catalyst was added and immediately subjected to light energy. A stop watch to note the time was started simultaneously. The beakers were removed at different time intervals 1, 2, 3, 4, and 5 hours and then the solutions analyzed for dye content.

CHAPTER FOUR

RESULTS AND DISCUSSION

4.1 Characterization of ZnO nanoparticles particles

The synthesized ZnO nanoparticle samples were taken for instrumental analysis in International Center for Research in Agro forestry (ICRAF) laboratories in Nairobi. ZnO nanoparticle samples were subjected to powder X-ray diffraction (PXRD) and Fourier Transform Infrared (FTIR) studies to determine the particle size and functional groups present respectively. The EDX and SEM analysis were also carried out in University of Western Cape, South Africa to determine elemental composition and morphology respectively.

4.2 Powder X-Ray Diffraction (PXRD)

The X-ray diffraction study of the samples was done by Philips X'pert model No. PW 3040/60 using Cu K α radiation ($\lambda=1.5060\text{\AA}$). The X-ray diffraction pattern of ZnO nano photocatalysts was recorded at 2θ angle. Figure 4.1 and 4.2 show the XRD patterns of the synthesized Zinc oxide nanoparticles and the standard JCPDS file 80-0075, respectively.

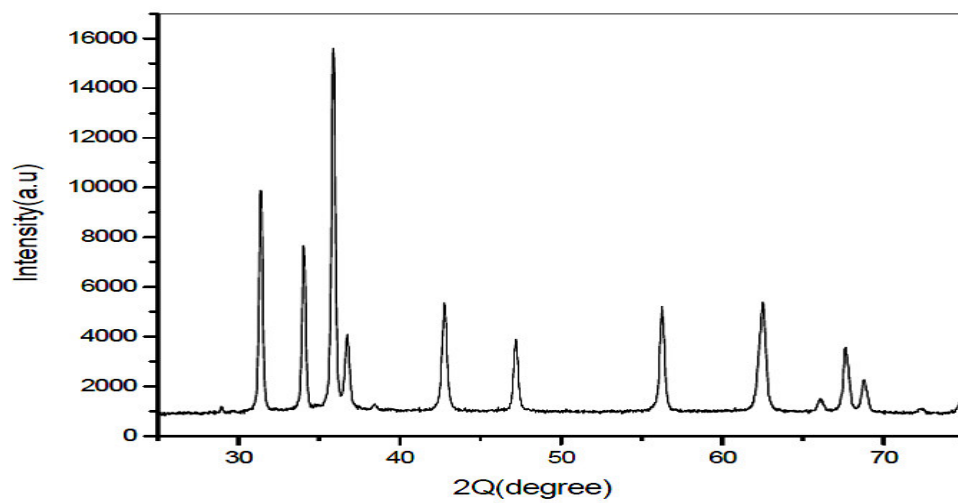


Figure 4.1: Observed Powder XRD pattern

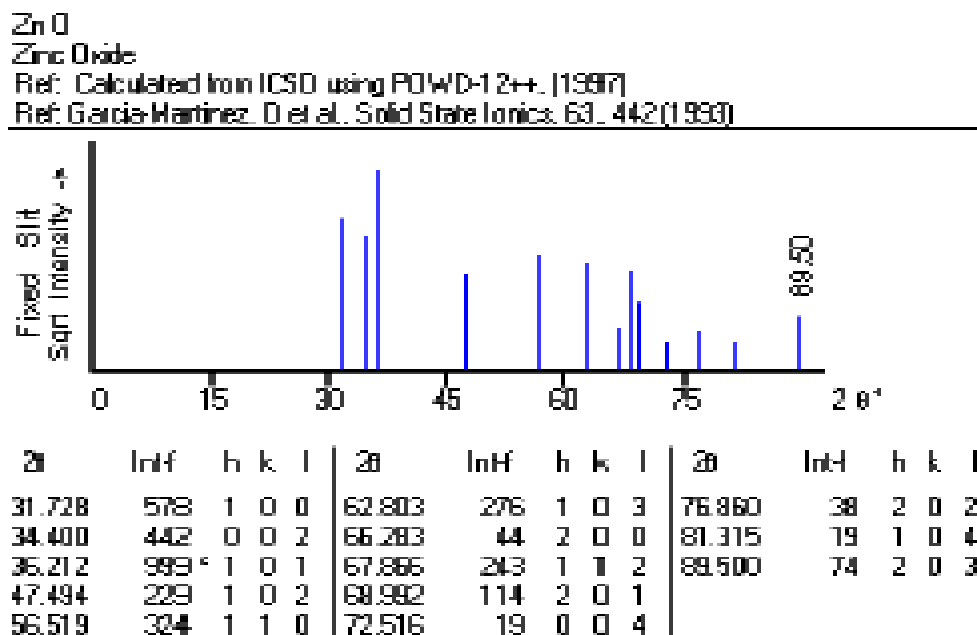


Figure 4.2: Reference JCPDS file 80-0075 for Wurzite ZnO

From figure 4.2, the diffraction peaks at 31.7, 34.4, 36.2, 47.4, 56.4, 62.5, 67.6, and 68.7 can be indexed to ZnO as per the JCPDS file 80-0075 as shown in Figure 4.1(b). Powder diffraction patterns are characteristic of a particular substance. It is its “fingerprint” and can be used to identify a compound. Powder diffraction data from known compounds have been compiled into a database by the JCPDS. The synthesized sample can be confirmed to be ZnO nanoparticle. Figure 4.1 (b) shows the reference JCPDS file that was used to visually compare (indexed) with XRD patterns obtained from the samples. Clear crystallinity of the ZnO nanoparticles was observed. The samples had

similar patterns. This suggests that the oxalic acid added as stabilizing agent had no effect on the wurzite structure of ZnO (Herrmann and Helmoltz, 2010).

Similar results were obtained by Gu *et al.* (2004) who obtained XRD peaks at scattering angles (2θ) of 31.3670, 34.0270, 35.8596, 47.1635, 56.2572, 62.5384, 67.6356, and 68.7978, corresponding to reflection from 100, 002, 101, 102, 110, 103, 200 and 112 crystals. They indexed the XRD patterns to ZnO nanoparticles reference JCPDS file 80-0075 as well.

The average crystallite size of ZnO nanoparticles was estimated according to the diffraction reflection by using Debye-Scherrer equation

$$T = \frac{0.9\lambda}{\beta \cos\theta} \text{-----15}$$

Where

λ - is the wavelength of incident X-ray (1.5406 Å)

β - Is the full width for half maximum (FWHM),

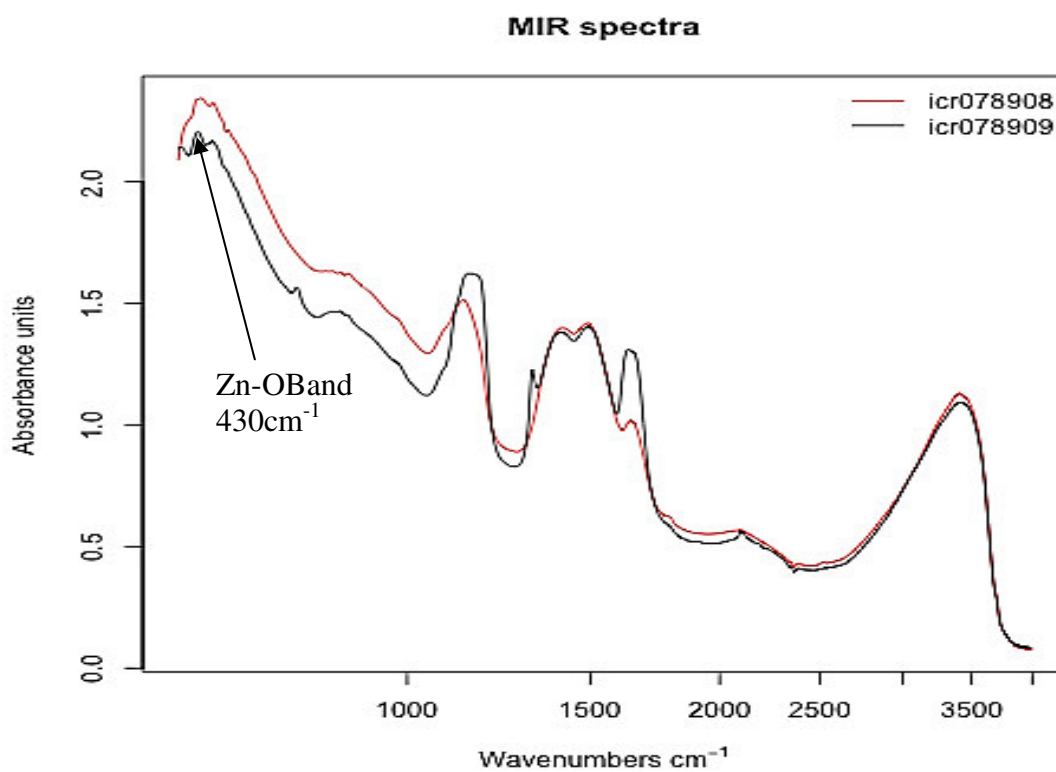
θ - is the Bragg's angle for the peak

β - Can be calculated using the equation $\beta = (2\theta_2 - 2\theta_1)$, obtained to be 0.2755 radians. The average crystallite sizes of synthesized ZnO nanoparticles were found to be around 26 nm. Similar results were obtained also by Shanthi and Muthuselvi (2012), who characterized synthesized nano-ZnO using PXRD. For their three samples prepared. The

sizes obtained were about 18nm, 16nm and 12nm.

4.2 The FTIR analysis

Figure.4.3 shows the FTIR spectrum of the synthesized ZnO nanoparticles synthesized by precipitation method, which was acquired in the range of 400-4000 cm^{-1} .



icr078908 – Sample 1

icr078909 – Sample 2

Figure 4.3: Observed FTIR pattern

FTIR of the ZnO nanocatalyst indicates the presence of water molecule adsorbed on the surface due to bands at around 3400 which may be assigned to OH stretching vibration of

adsorbed H_2O due to residual $\text{Zn}(\text{OH})_2$ present in the powder (Shanthi and Muthuselvi, 2012). The absorption band at 430cm^{-1} correlated to metal oxide bond (Zn-O).



Figure 4.4: Reference ZnO Spectra

Kant and Kumar (2012) carried out similar study, FTIR spectra of ZnO obtained showed absorption band at 432.0 cm^{-1} which they attributed to (Zn-O) stretching frequency. Likewise peaks at 3401.3 cm^{-1} represent (O-H) stretching mode. Shanthi and Muthuselvi (2012) also carried out a similar study and their analysis showed a broad band between $419\text{-}430\text{cm}^{-1}$. The spectra showed bands at (3250 and 3500cm^{-1}) which was assigned to O-H stretching vibrations.

4.3 SEM Analysis

Figure 4.5 and Figure 4.6 shows the SEM diagram for sample L₁ and L₂ at high magnification respectively.

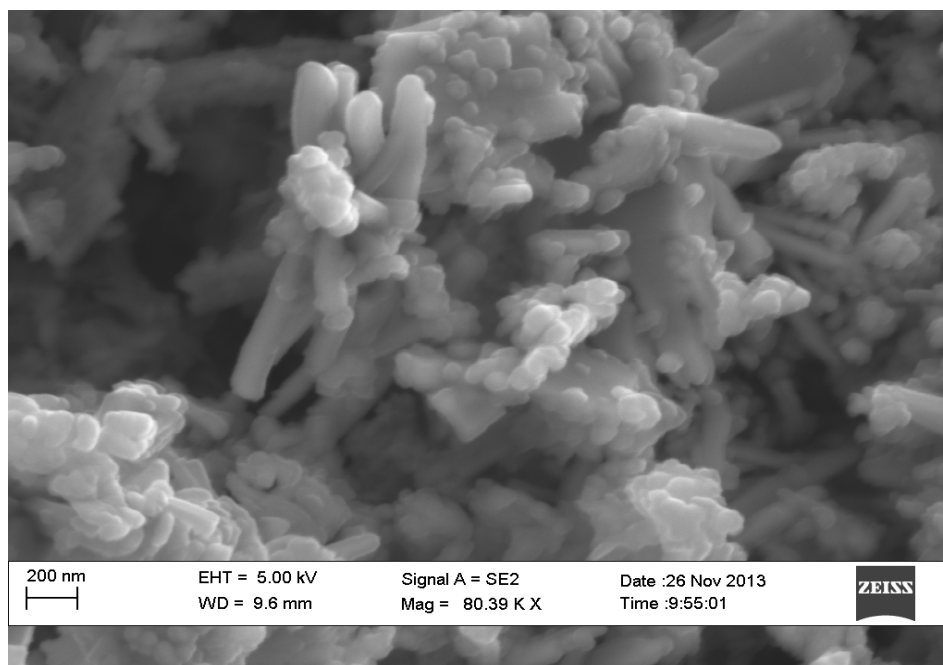


Figure 4.5: L₁ SEM diagram (Magnification = 80.39K X)

(Source: Author, 2015)

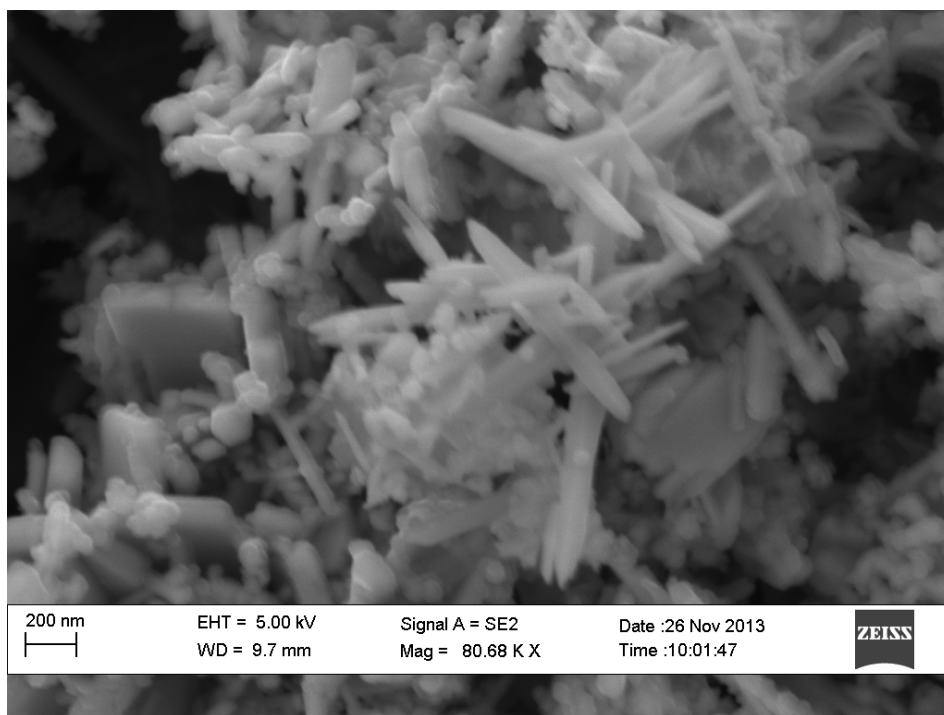


Figure 4.6: L₂ SEM diagram (Magnification = 80.68K X)

(Source: Author, 2015)

These images showed that the ZnO nanoparticles obtained formed rod shaped clusters distributed within the range of 200nm. The diagrams also show that the surface was not uniform but porous in nature. It shows that the nanocatalyst has considerable number of pores where there is a good possibility for the dye and heavy metals to be trapped and adsorbed onto these pores and it is a good sign for effective adsorption of dye and heavy metals (Joshi and Shrivastava, 2012).The photographs also showed different surfaces for

L₁ and L₂. The L₁ showed round ended while L₂ showed sharp ended nanoclusters. This showed that the stabilizing agent had an influence on the morphology of the samples.

Similar studies were made by Soltaninezhad and Amrnifar, (2011). They studied surface morphology of ZnO nanoparticles produced by Spray Pyrolysis. The pictures observed showed particles that were spherical in shape. However Joshi and Shrivastava, (2012) determined the surface texture which was found to be rough and porous in nature.

Also Shanthi and Muthuselvi, (2012) under a similar study, characterized nano ZnO synthesized by precipitation and the SEM pictures showed sphere and cube like nanoparticles which were distributed within the range of 100nm.

Due to these close similarities, the ZnO nanoparticles were confirmed. The difference in distribution range is attributed to the level of consistency during synthesis and also method of synthesis (Joshi and Shrivastava, 2012).

4.4 EDX Analysis

Figures 4.7 and 4.8 showed the EDX results for samples L_1 and L_2 , respectively.

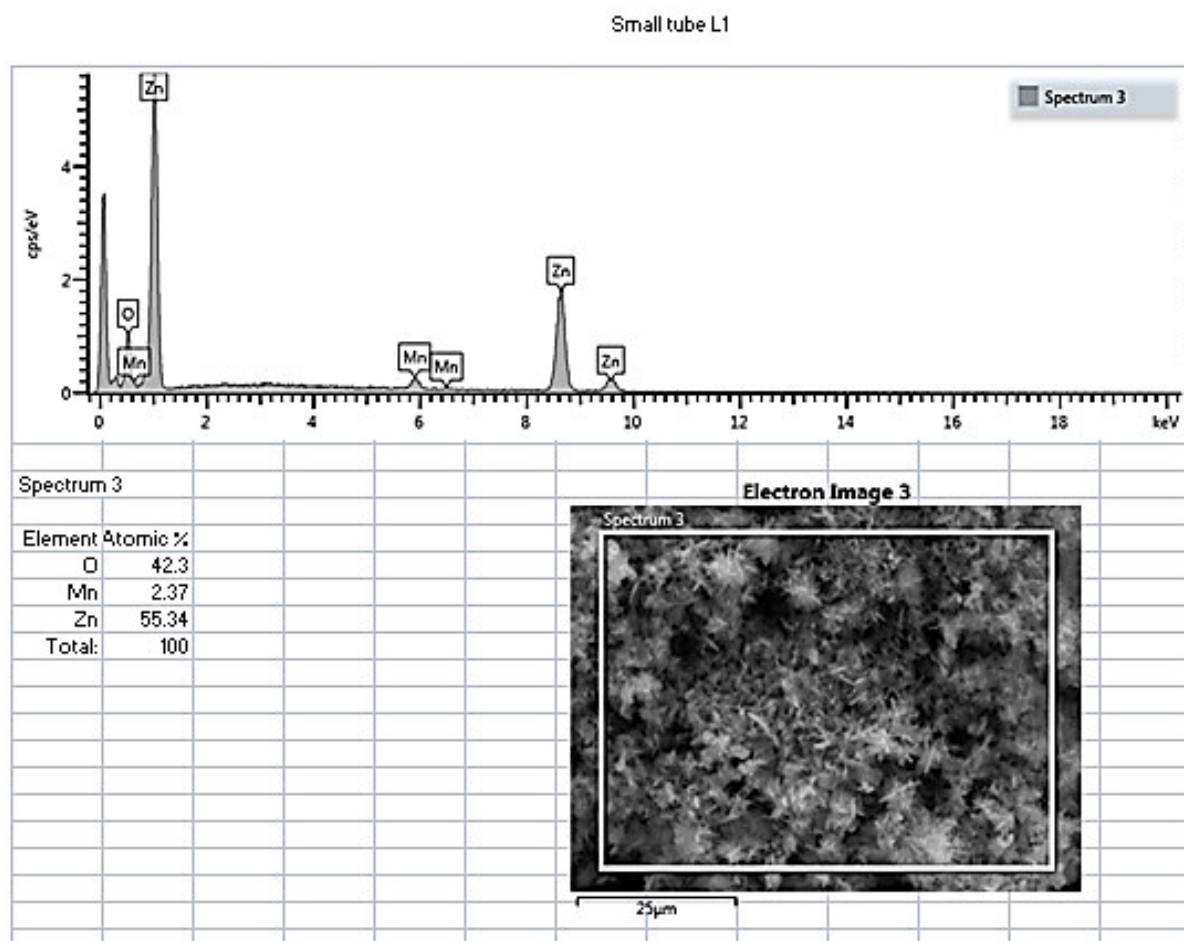


Figure 4.7: EDX Pattern ZnO L_1

(Source: Author, 2015)

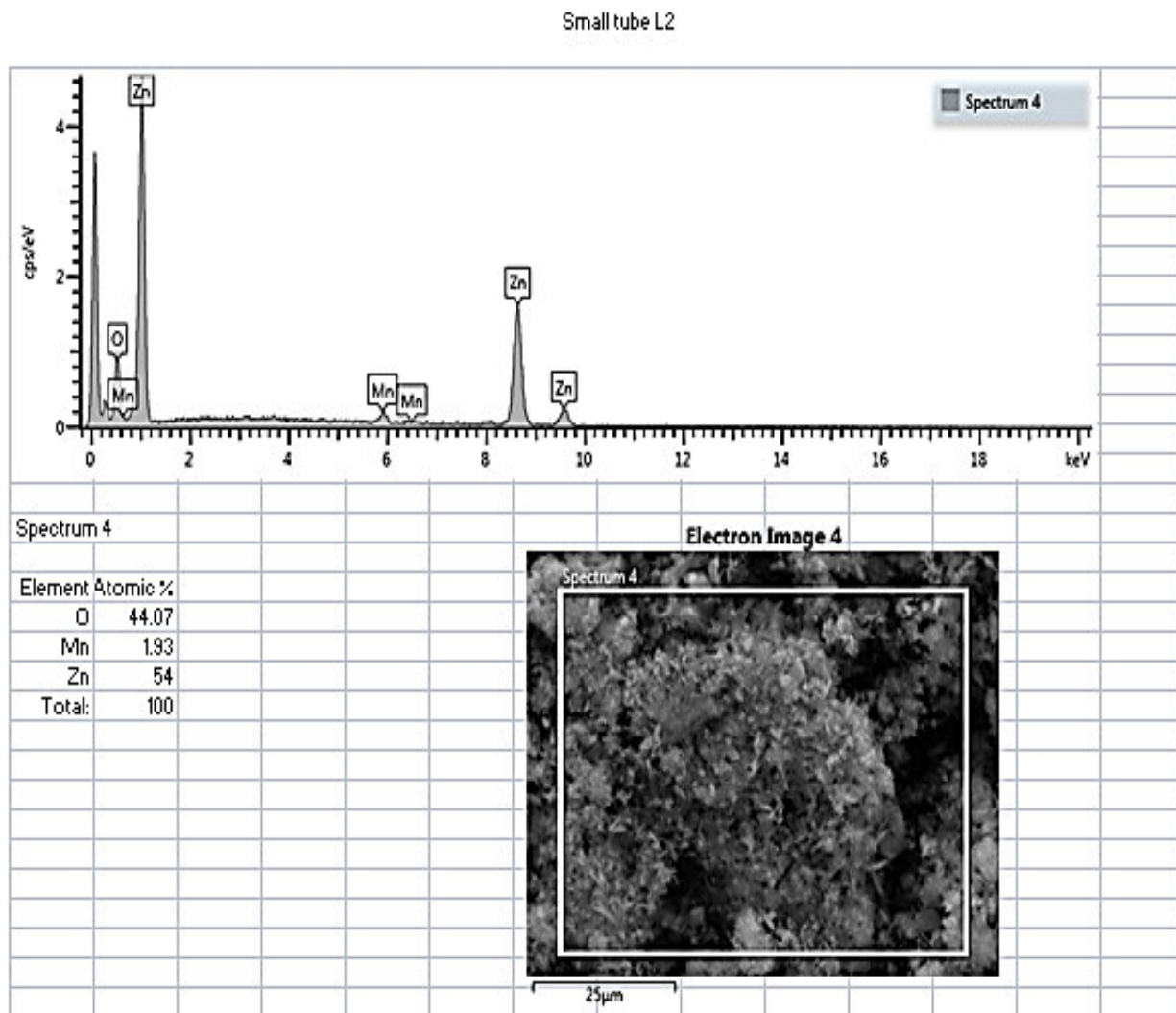


Figure 4.8: EDX Pattern ZnO L₂ (Source: Author, 2015)

The EDX spectra indicated that the samples were made up of Zn, O and traces of Mn impurities. The most intense peak is assigned to the bulk ZnO and the less intense one to the surface ZnO. The peak at 0.5 KeV can only be attributed to O and not Mn due to

overall position of the peaks. The elemental composition of the nanomaterial was found to be 55.34% Zn, 42.3% O and 2.37% Mn for L₁ and 54% Zn, 44.0% O and 1.93% Mn for L₂.

Similar work has been done by (Joshi and Shrivastava 2012) who characterized nano ZnO synthesized by precipitation technique. Their EDX spectra showed a peak at 0.5 Kev for oxygen 1 Kev for ZnL_α, 8.6 for ZnK_α and 9.6 Kev for ZnK_β. The elemental composition was found to be 71% Zn, 18.5% CO and 10% C with carbon as the impurity.

4.5 Heavy Metals Analysis

4.5.1 Effect of initial heavy metals concentration on Adsorption capacity of ZnO nanoparticles

To evaluate the capacities of ZnO to remove heavy metals, batch experiments were performed with fixed adsorbent dosage of 250 mg at various initial concentrations (100-400 mgL⁻¹) of heavy metal solution. The effect of the initial Cd²⁺, Ni²⁺ and Cu²⁺ concentration on the adsorption and adsorptivity (percentage of heavy metals adsorbed) is shown in figure 4.9.

Figures 4.9 – 4.11 were plotted using data in appendices 3, 4 and 5 respectively.

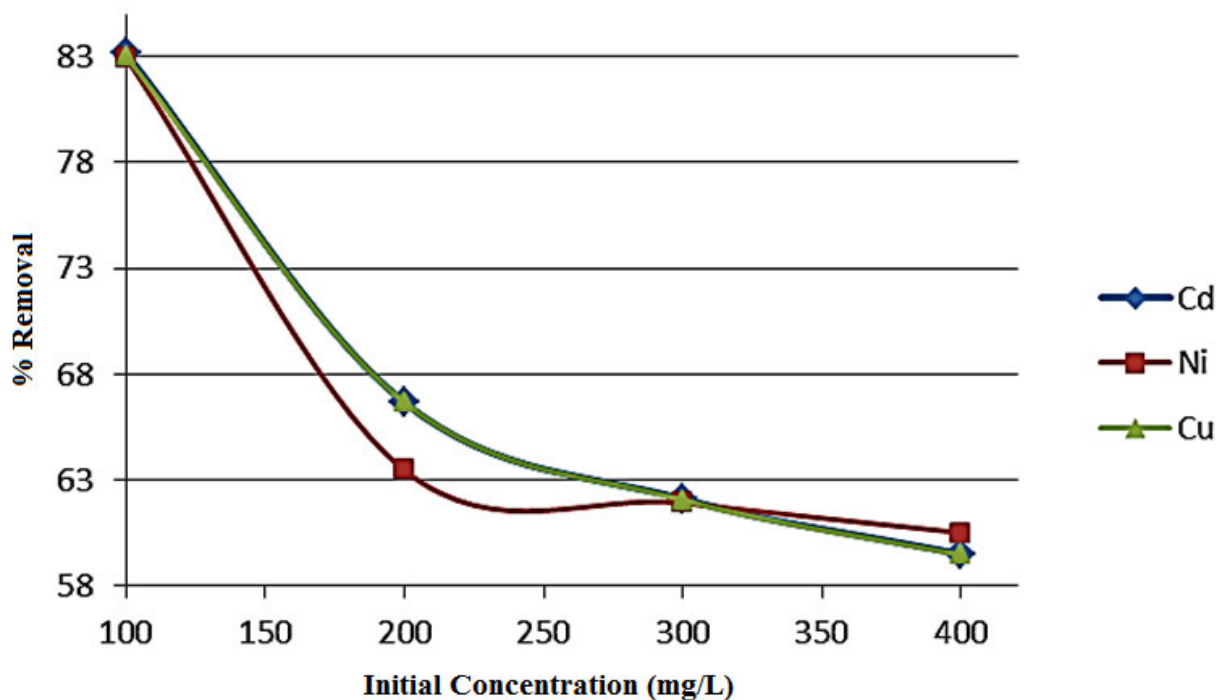


Figure 4.9: Effect of initial heavy metals concentration on adsorption capacity of ZnO nanoparticles

The adsorptivity decreased with increasing heavy metal concentrations. Further, sorbents active sites were saturated and further increase in the concentration would have no effect on the metal uptake. The maximal levels of uptake adsorption reached for ZnO were Cd(83.1%), Ni (82.9%) and Cu (83.0%) at initial concentration of 100 mgL⁻¹.

4.5.2 Effect of adsorbent dose on percentage removal of heavy metals

The adsorbent dosages were varied from 100mg to 500mg, while all the other variables such as contact time, pH and temperature were kept constant at 90 minutes, 7.0 and 25⁰C respectively and the results are shown in Figure 4.10.

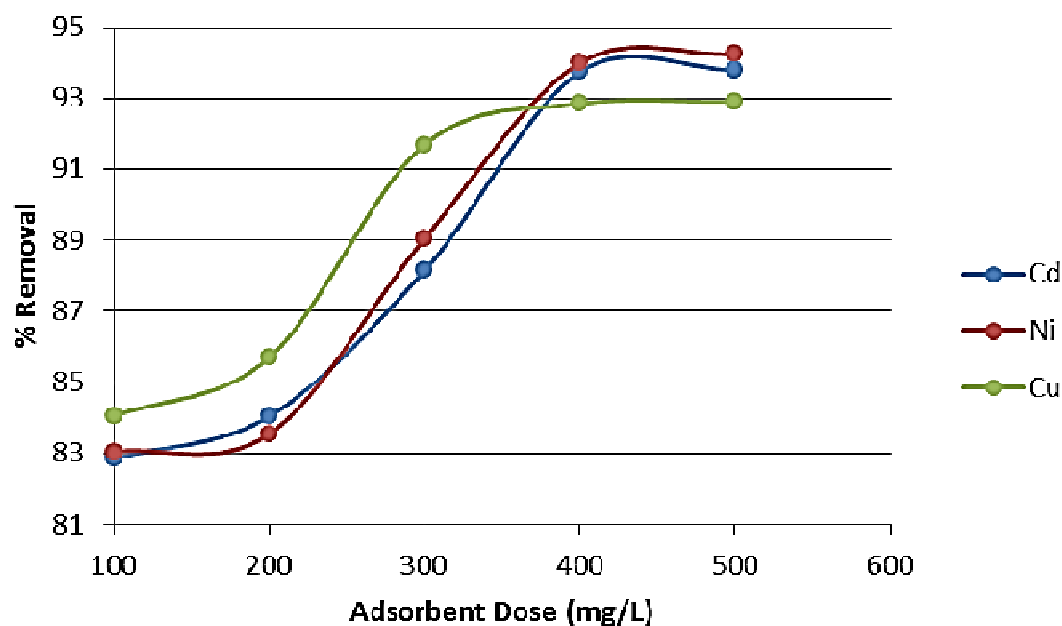


Figure 4.10: Effect of adsorbent dose on percentage removal of heavy metals

Adsorbent dose is an important parameter in the determination of adsorption capacity. As the adsorbent dosage increased from 100mg to 500mg, the adsorption sites available for heavy metal ions also increased and consequently better adsorption took place. For a fixed initial concentration of heavy metals, the amount of metal retained by gram of ZnO nanoparticles increased with the amount of ZnO nanoparticles (increase in the number of active sites). When more was added, retention was almost total. The same cations were

distributed on greater amount of surface and therefore resulted in reduction of adsorption amount on adsorbent (Kansal *et al.*, 2006).

The results agree with those found by Engates and Shipley (2011) who carried out a study to determine adsorption of Pb^{2+} , Cd^{2+} , Cu^{2+} and Ni^{2+} by ZnO nanoparticles, by studying adsorption of single and multi-metal ions by ZnO nanoparticles. They found a 100% removal efficiency of Pb^{2+} , Cd^{2+} and Ni^{2+} ions at 0.1 g L^{-1} within 120 min. of 50 mg, pH 8 and 24 hours contact time.

4.5.3 Effect of pH on Heavy Metal adsorption

The effect of pH on the surface species is responsible for the adsorption of ions from the solution. Effect of pH on the adsorption capacity of ZnO nano particles was evaluated by agitating 200 mgL^{-1} metal ion solution with 250 mg of ZnO for 90 minutes at pH ranging from 2, 4, 6 and 8. The quantities of heavy metals adsorbed on ZnO adsorbent was represented in figure 4.11

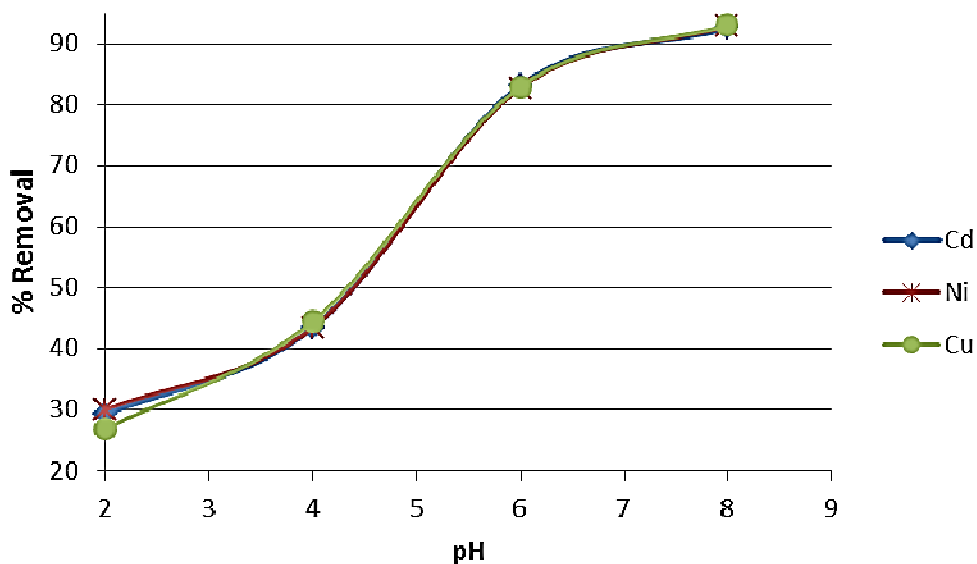


Figure 4.11: Effect of pH on ZnO nano particles heavy metals adsorption

The results on adsorption percentages of Cd^{2+} , Ni^{2+} , and Cu^{2+} at pH 2 showed that the maximum amount adsorbed was; Cd^{2+} (28.5 %), Ni^{2+} (29.1%) and Cu^{2+} (26.5%). Increasing the pH to 8, the adsorbed amounts were; Cd^{2+} (92.1%), Ni^{2+} (92.8%) and Cu^{2+} (92.0) as shown in Figure 4.11. The results agree with Yuan *et al.* (2013) who found that adsorption of metal ions (Pb^{2+} , Cu^{2+} and Cd^{2+}) gradually increased with an increase of the pH of the medium, and maximum removal efficiency was observed at pH 8.

The results suggest that at high pH the surface charge of ZnO nanoparticles is more negative due to presence of OH groups that leads to formation of hydroxyl complexes. Formation of such hydroxyl compounds at higher pH is responsible for the uptake of the metal ions from solution. In contrast, the low degree of sorption at low pH can be

attributed to the competition of cations (metal ions) and protons (H^+) for the same sites, as well as the repulsion between ions of the same surface charge (Kumar *et al.*, 2013).

4.6 Photo-catalytic degradation studies

The optical density of each dye was measured using UV-VIS spectro-photometer at maximum wavelength of 480 nm. A plot of optical density versus initial concentration is shown in Figure 4.12. This plot was used as standard graph for estimation of dye concentration by interpolation technique.

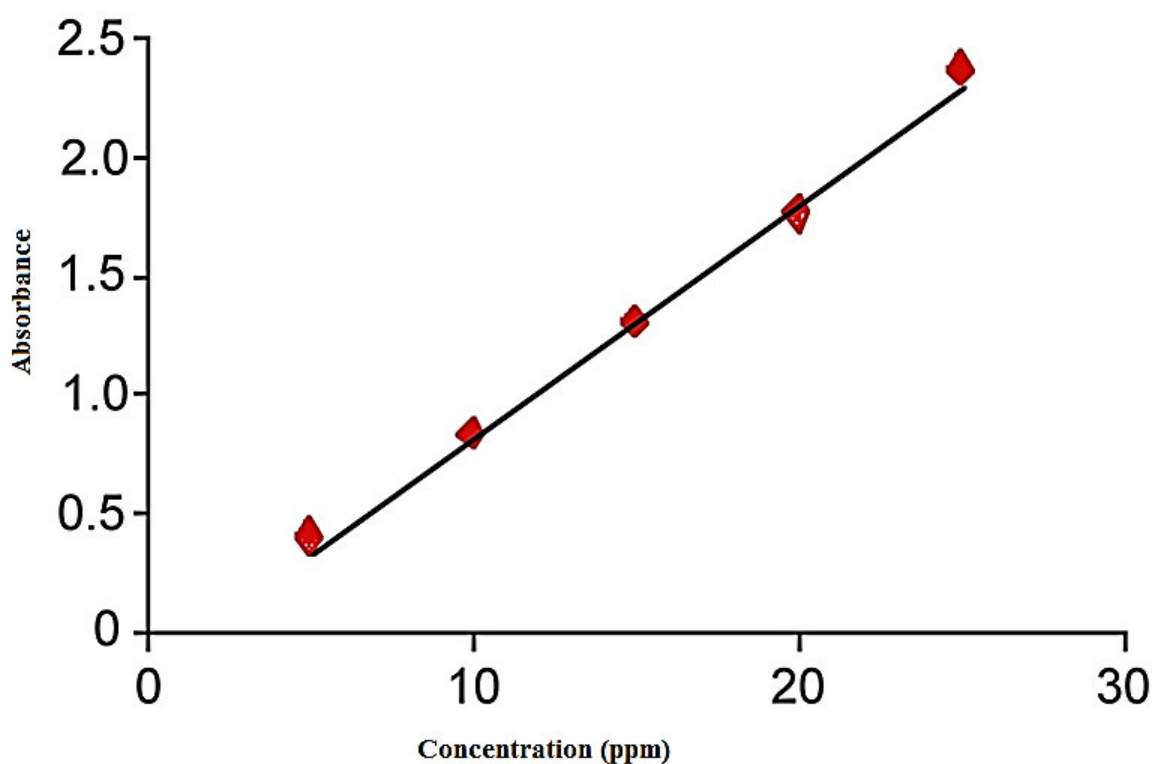


Figure 4.12: Standard curve for methyl orange dye

4.6.1 Effect of variation of initial concentration of dye on photo degradation of methylorange dye

Table 4.1 shows the effect of variation of initial concentration of Methyl orange dye on photodegradation.

Table 4.1: Effect of variation of initial concentration of dye on photo degradation of methyl orange dye

Radiation	Sample	Concentration of dye		
		15 mgL ⁻¹	30 mgL ⁻¹	45 mgL ⁻¹
Sunlight	L ₁	0.85	2.68	10.77
	% removal	98.4%	96.1%	94.7%
	L ₂	2.49	6.83	20.89
	% removal	97.4%	97.2%	93.6%
Fluorescent	L ₁	14.23	26.40	41.31
	% removal	92.0 %	89.0%	88.2%
	L ₂	14.04	29.81	38.03
	% Removal	91.8%	88.9%	88.0%

Photo catalytic degradation of the dye was found to decrease with increase in initial concentration of methyl orange. This could be due to more dye molecules than ZnO nanoparticles; in this case the photo-catalyst became the limiting factor. It was noted that degradation rate decreased with increase in dye concentration. The decrease in dye degradation could be attributed to reduction of OH[•]radicals on the catalyst

surface when covered by dye ions (Poulis and Tsachpinis, 1999). Appendices 1 and 2 shows photodegradation based on contact time.

The results are similar to those reported by Li *et al.* (2005) when methyl orange was irradiated with sunlight source, the degradation of the dye decreased as the dye concentration increased. This due to the fact that the generation of OH radical on the catalyst surface is reduced since the active sites are covered by dye ions. Also Kansal *et al.* (2006) concluded that photo-catalytic degradation of methyl orange decreased as the dye concentration increased.

This decrease is as a result of increasing the number of photons absorbed by catalyst lower concentration (Davis, 2006). According to Shanthi and Muthuselvi (2012), the decrease in photo degradation is as a result of dye molecules imparting darker colour to the solution which acts as a filter to the incident light reaching the photo catalyst surface. Sampa and Biney (2004) further explained that the increase in the concentration of a dye solution result in the photons getting intercepted before they can reach the catalyst surface, thus decreasing the absorption of Photons.

4.6.2 Effect of variation of dose of photocatalyst (L_1 and L_2) on photo degradation of MeO dye

The initial concentration 30 mgL^{-1} of the dye and pH in all beakers were kept constant at pH 7.0 and the dose of photo-catalyst was varied from 200 mg to 400mg with a contact time of four hours and the results are shown in Table 4.2.

Table 4.2: Effect of variation of dose of photo catalyst (L₁ and L₂) on photo degradation of MeO dye

Radiations	Sample	Amount of photo-catalyst		
		200mg	300mg	400mg
Sunlight	L ₁	6.57	2.39	1.50
	% removal	92.1	94.2	96.0
	L ₂	10.99	6.83	4.06
	% removal	93.4	97.2	96.5
Fluorescent	L ₁	26.40	26.88	26.55
	% removal	92.0	96.4	98.5
	L ₂	29.81	27.46	25.23
	% removal	92.6	97.5	97.9

Photo catalytic degradation of methyl orange dye increased with an increase in concentration of ZnO particles. This is due to increase in photocatalyst molecules available to degrade the dye. Further increase of ZnO nanoparticles concentration increase turbidity of the solution and decreases light penetration into the solution and therefore, removal efficiency decreases (Kartalet *al.*, 2001).

The results of this study are similar to those of Joshi and Shrivastava (2012) who studied removal of methylene blue using ZnO nano particles, by varying the dose of photo catalyst from 2.0 g/l to 5.0 g/l and degradation increased from 86.0% to 92.8% as shown in Table 4.2. The increase in the amount of catalysts increased the number of active sites

of the photo catalyst surface, which in turn increased the number of hydroxyl and superoxide radicals (Sampa and Biney, 2004).

4.6.3 Effect of variation of contact time on photo degradation of MeO dye

The results are presented in Table 4.3 below.

Table 4.3: Effect of variation of contact time on photo degradation of MeO dye

<i>Radiations</i>	<i>Sample</i>	<i>Contact time in hours</i>				
		1	2	3	4	5
Sunlight	L ₁	11.84	6.83	5.99	1.45	0.58
	% removal	60.5	77.2	80.0	95.2	98.0
	L ₂	9.12	4.23	2.68	0.97	0.53
	% removal	69.6	85.9	91.1	96.8	98.2
Fluorescent	L ₁	10.95	8.77	5.95	2.68	1.32
	% removal	63.5	70.8	80.2	91.1	95.6
	L ₂	11.57	8.15	5.33	2.06	0.70
	% Removal	61.4	72.8	82.2	93.1	97.7

The mixture of L1 and L2 affects percentage removal of MeO which is higher than non-stabilized and lower than the stabilized as indicated in appendices 1 and 2.

The results indicated that, the percentage removal of dye increases with increase in contact time. This is in agreement with the results reported by Shanthi and Muthuselvi,(2012), who studied the effects of contact time on removal of malachite green using ZnO nano particles. The increased contact time causes the photogenerated

OH radicals and other peroxide radicals all being highly oxidant species decompose the dyes completely to mineral end products (Hofman, 2005).

4.7 Equilibrium isotherm models for photo degradation of MeO dye using sunlight

Two isotherm models were tested in the present study and these are Langmuir and Freundlich. The applicability of the isotherm equation is compared by judging the correlation coefficient R^2 (Fytianos *et al.*, 2000). Langmuir theory was based on the assumption that adsorption was a type of chemical combination or process and the adsorption layer was unimolecular (Samarghadi *et al.*, 2009).

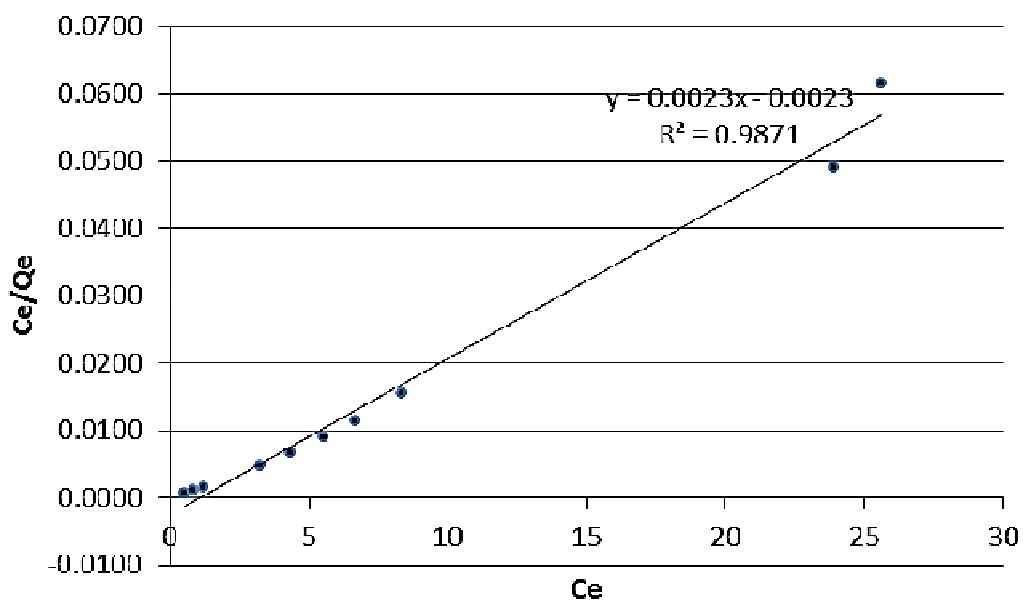


Figure 4.13: Langmuir adsorption isotherm of methyl orange adsorption

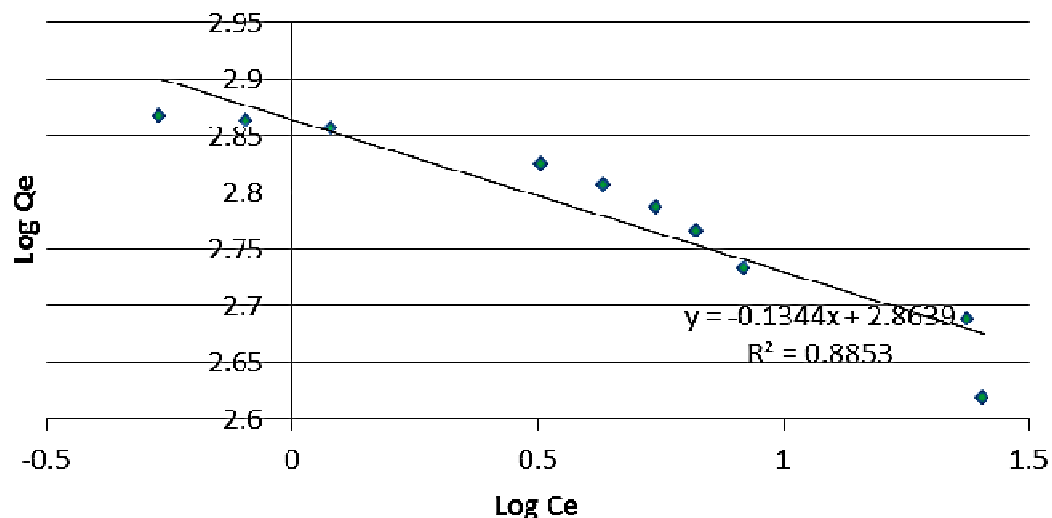


Figure 4.14: Freundlich adsorption isotherm of methyl orange adsorption

Figures 4.13 to 4.16 were plotted from appendices 3, 4, 8 and 9. The coefficient of correlation for ZnO nanoparticles obtained from figure 4.13 for Langmuir expression ($R^2 = 0.9871$) and ZnO coefficient of correlation obtained from figure 4.14 for Freundlich expression ($R^2 = 0.8853$) indicated that Langmuir expression provided better fit for the experimental data of photocatalytic degradation of methyl orange using ZnO nanoparticles than Freundlich expression.

These findings are in agreement with those of a study conducted by Joshi & Shrivastava (2012) on degradation of alizarine red-s (a textiles dye) by photocatalysis using ZnO and TiO₂ as photo-catalyst. In their study, the good fit for the experimental data and the correlation coefficients R^2 higher than 0.9996 indicated the applicability and suitability of Langmuir isotherm model more than the Freundlich isotherm.

4.8 Equilibrium isotherm models for photo degradation of MeO dye using florescent

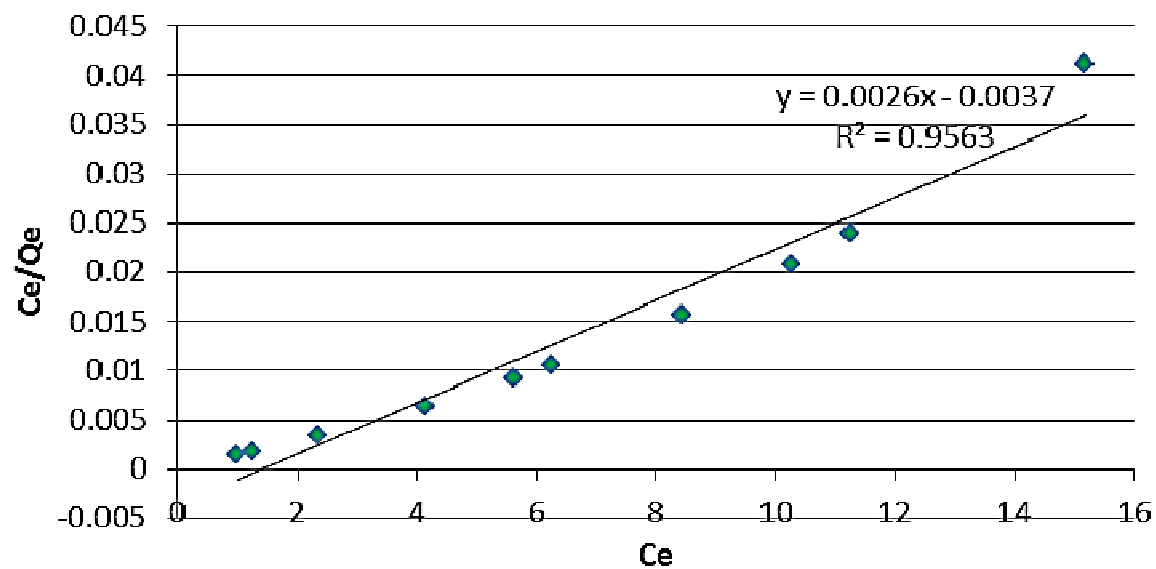


Figure 4.15: Langmuir Isotherm for photo degradation of MeO dye using florescent

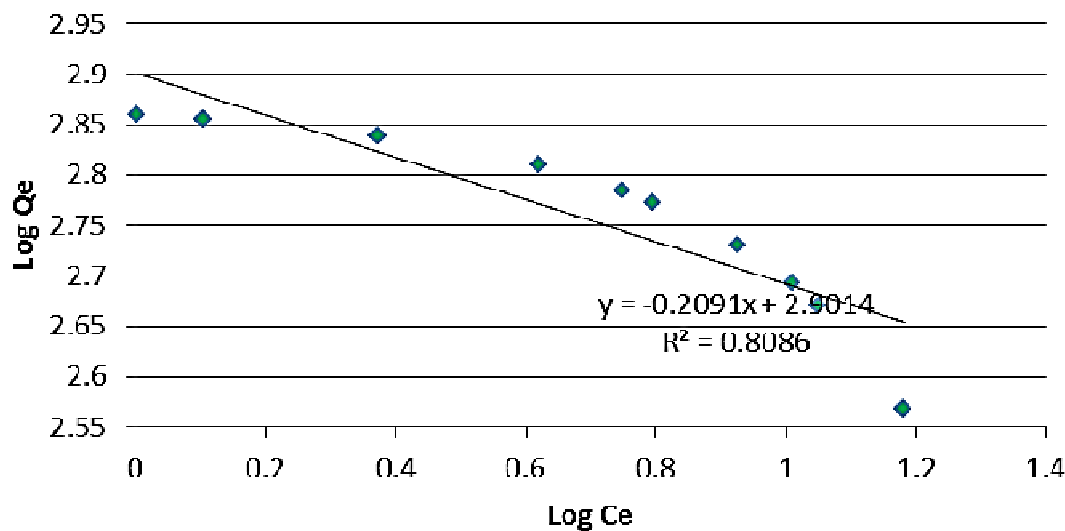


Figure 4.16: Freundlich Isotherm for photo degradation of MeO dye using fluorescent

The coefficient of correlation for ZnO nanoparticles obtained from figure 4.15 for Langmuir expression ($r^2 = 0.9563$) and ZnO coefficient of correlation obtained from figure 4.16 for Freundlich expression ($r^2 = 0.8086$) indicated that Langmuir expression provided better fit for the experimental data of photocatalytic degradation of methyl orange using ZnO nanoparticles under fluorescent than Freundlich expression.

These findings are in agreement with the findings of study conducted by Samarghandi *et al.* (2009), on two-parameter isotherms of methyl orange sorption using pinecone derived activated carbon. In their study, the good fit for the experimental data and the correlation coefficients r^2 higher than 0.9271 indicated the applicability and suitability of Langmuir isotherm model more than the Freundlich isotherm (0.5893).

4.9 Adsorption kinetics for photo degradation of MeO dye using sunlight

For the evaluating the adsorption kinetics of methyl orange on ZnO nanoparticles, the data was treated with Lagergren first order model expressed as

-----16

The first order rate constant k_1 is obtained from the slope of the plot $\log (q_e - q_t)$ versus time,

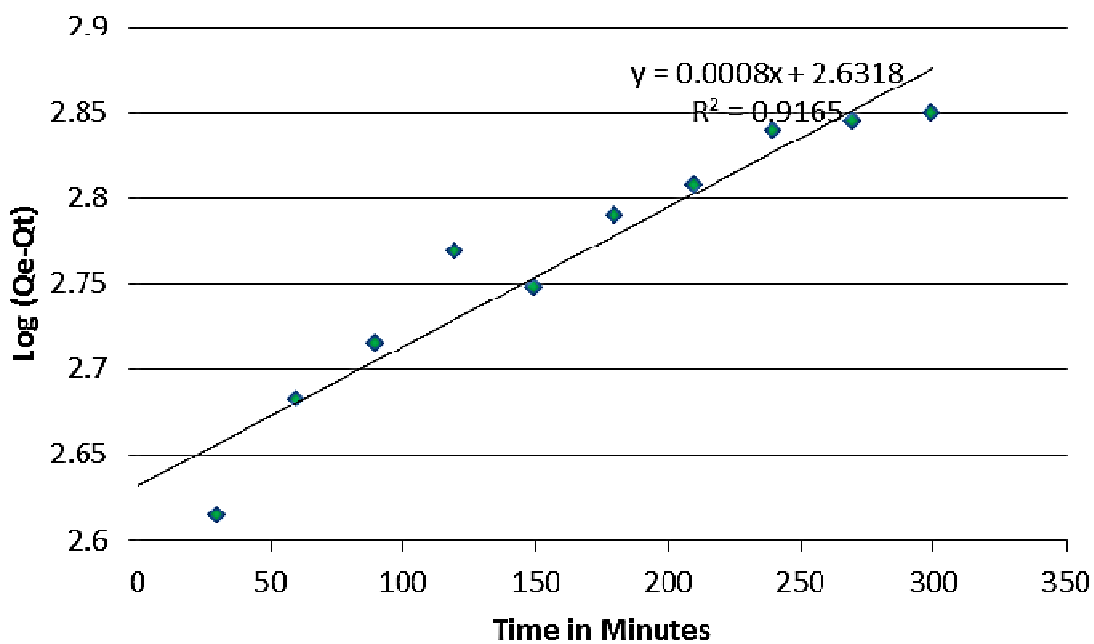


Figure 4.17: Lagergren first order plot of methyl orange degradation under sunlight

Adsorption kinetics were also explained by the pseudo second order model (Yuh-Shan, 2004)

where K_2 is the second order rate constant ($\text{g mg}^{-1}\text{min}^{-1}$). The value of K_2 is different initial dye concentration for all adsorbents which were calculated from the slope of the respective linearplot of t/qt vs t .

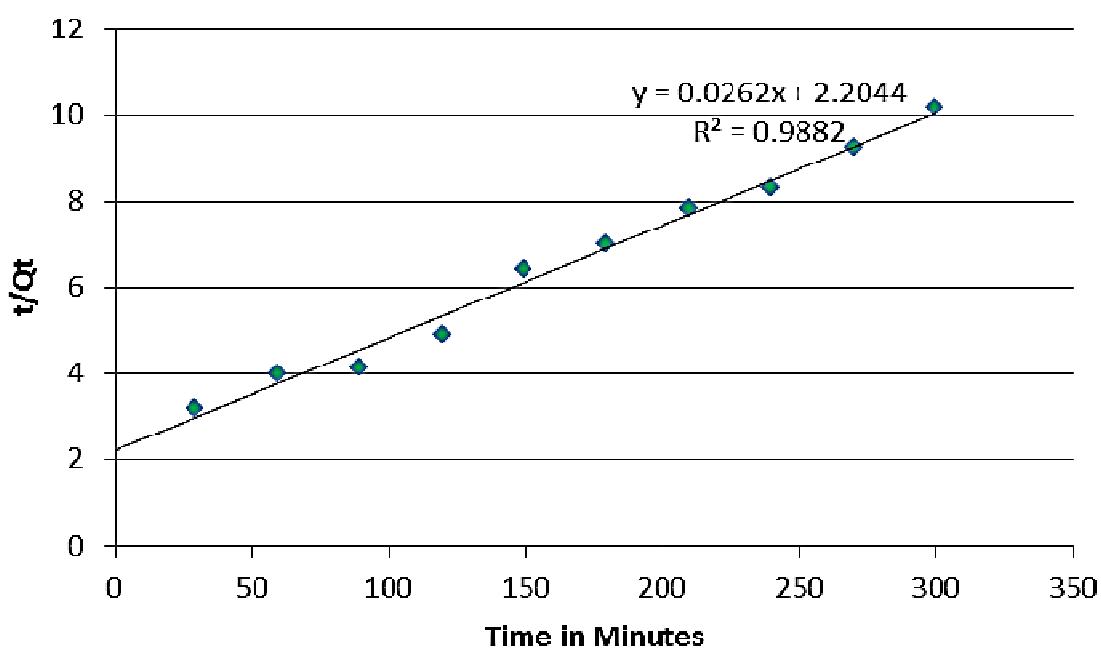


Figure 4.18: Lagergren second order plot of methyl orange degradation under sunlight

The correlation coefficients from figures 4.15 and 4.16 for these two tests ranged from 0.9165 for the first order kinetics to 0.9882 for the second order kinetics. This suggests that there existed a strong relationship between the parameters and also that the process

followed the pseudo second order kinetics figure 4.16. This shows that the degradation process of methyl orange on ZnO nanoparticles followed pseudo second order kinetics. These findings are in agreement with those of Joshi & Shrivastava (2012) who conducted a study on the degradation of alizarine textile dye by photocatalysis using ZnO and TiO₂ as photocatalyst. For their study, the correlation coefficients were 0.9946 and 0.9998 for first order and second order, respectively suggesting a strong relationship between the parameters and also explaining that the process followed the pseudo second order kinetics.

The findings also correlate with the findings of Sampa and Biney (2004) who conducted a study on photo-catalytic degradation of modern textile dyes in waste water using ZnO nanocatalyst. For their study, the correlation coefficients were 0.9849 and 0.9988 for first order and second order, respectively, suggesting a strong relationship between the parameters and also explaining that the process followed the pseudo second order kinetics.

4.10 Adsorption kinetics for photo degradation of MeO dye using fluorescent

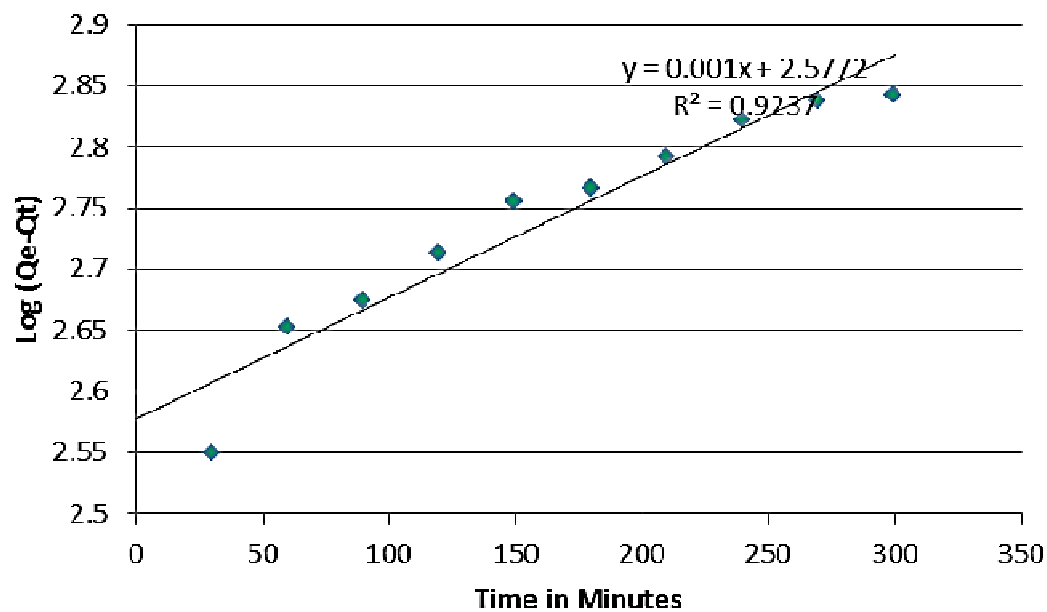


Figure 4. 19: Lagergren first order plot of methyl orange adsorption under fluorescent illumination

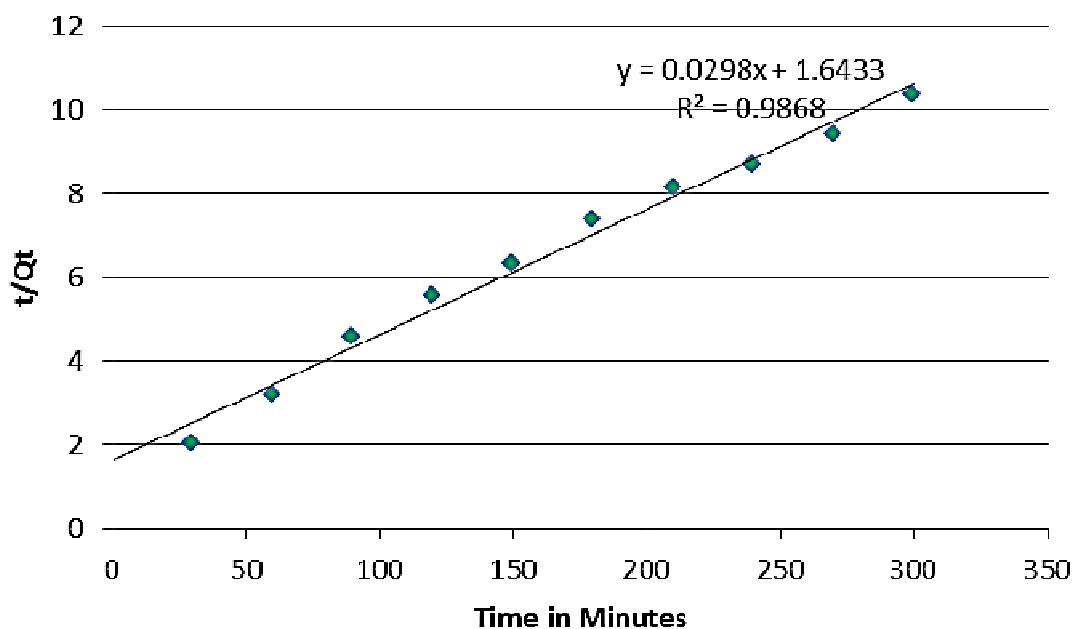


Figure 4. 20: Lagergren second order plot of methyl orange adsorption under fluorescent illumination

The correlation coefficients from figures 4.19 and 4.20 for these two tests ranged from 0.9237 for the first order kinetics to 0.9868 for the second order kinetics. This suggests that there existed a strong relationship between the parameters and the process followed the pseudo second order kinetics figure 4.19. This shows that the adsorption process of methyl orange on ZnO nanoparticles under florescent follows pseudo second order kinetics.

These findings are in line with those of Jalilet *al.* (2010) who conducted a study on the adsorption of methyl orange from aqueous solution onto calcined lapindo volcanic mud under fluorescent conditions. For their study, the correlation coefficients were 0.9643 and

0.9898 for first order and second order respectively, suggesting a strong relationship between the parameters and that the process followed the pseudo second order kinetics.

4.11 Comparison of Adsorption Efficiency of ZnO nanoparticles

The findings clearly showed that increased adsorption power was evidenced when the photocatalyst was enhanced using a stabilizer. The difference in adsorption was minor but appreciable. This could be attributed to the fact that the oxalic acid used is a capping agent which provided protective organic shell to particles to prevent the nanoparticles from aggregating in solution. It also promotes formation of fewer, larger nuclei and thus nanocrystal particle sizes (Gnanasangeetha and Sarala, 2013). Stabilizers enable the nanoparticles to be resistant to deactivation and thus its performance which depends on the nature and concentration of the stabilizing agent used (Gnanasangeetha and Sarala, 2013).

In addition, the use of sunlight as a source of radiation was found to give better results than fluorescent light. Adsorption of heavy metals and photodegradation of methyl orange by the nanoparticles was found to be more efficient when done under sunlight than when performed under fluorescent light. This is attributed to the fact that sunlight intensity is higher than that of fluorescent light. Increase in intensity increases the number of photons reaching the adsorbent and thus its adsorption and photo degradation ability.

CHAPTER FIVE

CONCLUSION AND RECOMMENDATIONS

5.1 Conclusion

The XRD results of the synthesized sample were confirmed to be for ZnO nanoparticle. The size of ZnO nanoparticles were found to have an average crystal size of 26 nm which is within the range of 1-100nm for nanoparticles. The FTIR spectrum of the synthesized ZnO nanoparticles synthesized was in the range of 400-4000 cm^{-1} . The band range of 430 cm^{-1} correlated to zinc oxide bond (Zn-O).

The adsorptivity of ZnO nanoparticles was found to decrease with increase in heavy metals concentrations, this indicates that sorbents active sites were saturated and further increase of the concentration will have no effect on the uptake. The maximal levels of uptake adsorption reached for ZnO nanoparticles were Cd^{2+} (83.1%), Cr^{2+} (82.9%) and Cu^{2+} (83.0%) at initial concentration of 100 mgL^{-1} and contact time of 90 minutes. Increase in adsorbent dosage increased adsorption percentage for the three metal ions.

At pH 2, the maximum amounts adsorbed were; Cd^{2+} (28.5 %), Cr^{2+} (29.1%) and Cu^{2+} (26.5%). Increasing the pH to 8, the adsorbed amounts were; Cd^{2+} (92.1%), Cr^{2+} (92.8%), and Cu^{2+} (92.0).

Photodegradation can be used for treatment of industrial effluents containing heavy metals and dyes. In place where we have plenty of sunlight solar radiation can be used for degradation.

Also we are using minute quantities of ZnO nanoparticles and there will be no harm in mixing this small quantity of Zn in water streams. As Zn is one of the essential trace elements. These results will be helpful in designing effluent treatment plants in industries.

5.2 Recommendations

In future, researchers should focus on the development of novel nanomaterials/nanocomposites with a high surface area, sufficient surface functional groups and high sorption ability, for the removal of different heavy metal ions and organic dyes. The microbial threats to human health and safety are also a serious public concern. Thus, further improvements must be made in the direction of the development of materials with greater stability (resistance to pH changes and concentrations of chemicals present in contaminated water) and the capacity for the simultaneous removal of multiple contaminants, such as toxic metal ions, organic dyes and bacterial pathogens.

Considering the economics of adsorbents, it is necessary to synthesize low-cost effective and recyclable adsorbents for their extensive application in our daily life. Treatment technologies should be developed for the purification of water in order to meet the demand of increased environmental pollution.

REFERENCES

- Akoh, C. C., Chang, S. W., Lee, G. C., & Shaw, J. F. (2007). Enzymatic approach to biodiesel production. *Journal of Agricultural and Food Chemistry*, 55(22), 8995-9005.
- Apiratikul, R. Pavasant, P. (2008). Sorption of Cu,²⁺ Cd,²⁺ and Pb²⁺ using modified zeolite from coal fly ash, *Chem. Eng. J.* 144 245–258.
- Awitor, K., Rafqah, S., Gérontona, G., Sibaud, Y., Larson, P., Bokalawela, R., Jernigen, J. and Johnson, M. (2008). Photo-catalysis using titanium dioxide nanotube layers. *Journal of Photochemistry and Photobiology A: Chemistry*, 199, 250 – 254.
- Ayuso, E.A., Sanchez, A.G. and Querol, X. (2003). Purification of metal electroplating waste waters using zeolites. *Water Research* 37, 4855-1862.
- Baouer, C.H., Jacques, P., and Kalta, W. (2001). Photo oxidation of an azo dye induced by visible light on the surface of TiO₂, *J photo chem. Chemistry*, 140, 87-92
- Binks, P. (2007). *Nanotechnology and water: opportunities and challenges*. Victorian Water Sustainability Seminar.
- Bellona, C. and Drewes, J.E. (2007). Viability of a low-pressure nanofilter in treating recycled water for water reuse applications: A pilot-scale study. *Water Research*, 41, 3948-3958.
- Bhattacharyya, K.G. Gupta, S.S. (2008). Influence of acid activation on adsorption of Ni(II) and Cu (II) on kaolinite and montmorillonite: *Kinetic and thermodynamic study*, *Chem. Eng. J.* 136, 1–13.
- Chumming, J. (2003). *Growth and characterization of ZnO and ZnO-based Alloys-MgxZn1-xO and MnxZn1-xO* PhD thesis, Department of materials science and Engineering, North Carolina state university, Raleigh.
- Davis J.C. (2006). *Managing the effects of nanotechnology*. Woodrow Wilson International Centre for Scholars, National institutes of health, Washington D.C., USA
- Daneshvar, N., Salari, D., Niaei, A.G. and Rasouli, F.M.H. (2004). *Immobilization of Titanium Dioxide on Glass Beads and Photocatalytic degradation of Malachite green under UV radiation*, Tehran, Iran
- Dann, E.S. (2000). *Characterization of solids*, Loughborough University

- Derjaguin, B.V. (1954). Investigations of the forces of interaction of surfaces in different media and their application to the problem of colloid stability. *Discussion of the Faraday society*, 18, 24 – 27.
- Drexler, E. (1986). Engines of creation. *The coming era of nano technology*. Massachusetts institute of technology. U.S.A
- Duffus, J.H. (2002). Heavy Metals”—A Meaningless Term? *Pure and applied chemistry*, 74 793-804
- Dupont, L. and Guillon, E. (2003). Removal of hexavalent chromium with a lignocellulosic substrate extracted from wheat bran. *Environmental Science and Technology*, 37, 4235 – 4241.
- Ellis, T.G. (2004). *Chemistry of waste water*. Eolss publishers, Oxford, UK.
- Engates, K. E. and Shipley, H. J. (2011). Adsorption of Pb, Cd, Cu, Zn, and Ni to ZnO nanoparticles: effect of particle size, solid concentration, and exhaustion. *Environ. Sci. Pollut. Res.* 18: 386–395.
- Feynman, R. (1959). *There's plenty of room at the bottom*. Available at: www.its.caltech.edu/~feynman/plenty.html.
- Fleischer, T. and Grunwald, A. (2008). Making nanotechnology developments sustainable. A role for technology assessment. *Journal of Cleaner Production*, 16, 889-898.
- Flemming, C., Baker, K., and Macintosh, C. (1991). *Analysis of chloro carbon in waste water*. Division of environmental chemistry, American Chemical Society. Atlanta
- Fytianos, K., Voudrias, E., & Kokkalis, E. (2000). Sorption–desorption behaviour of 2, 4-dichlorophenol by marine sediments. *Chemosphere*, 40(1), 3-6.
- Gnanasangeetha, D. and Sarala Thambavani, D. (2013). One Pot Synthesis of Zinc Oxide Nanoparticles via Chemical and Green Method, *Research Journal of Material Sciences*, 1(7), 1-8
- Goldstein, J. I., (2003). *Scanning Electron Microscopy and X-ray Microanalysis*, 3rd ed, Plenum Press, New York.
- Gregorio, C. (2006). Non-conventional low-cost adsorbents to dye removal. *A review Bioresource Technology*, 97, 1061 – 1085.
- Gribbin, J. (1997). *Richard Feynman: A Life in Science*. Dutton, p 170.

- Gu F., Wang S.F., Lu M.K., Zhou G.J., Xu D., and Yuan D.R. *Langmuir*, (2004) 20: 3528.
- Herrmann, V. and Helmoltz, P. (2010). Influence of stabilizers in ZnO nanodispersions on the performance of the nano particles. *Phys Status Solid*, 207(7), 1684 – 1688
- Hillie, T. and Munasinghe, M. (2006). *Nanotechnology, water and development*. Global Dialogue on Nanotechnology and the Poor: Opportunities and Risks, Meridian Institute.
- Hoffman, A. (1995). Shades of green. *Stanford Soci. Innov. Rev.*, Spring: 40–49.
- Howe, C. and Macintosh, P. (1991). *The use of Fourier Transform Spectroscopy in Combustion Effluents Monitoring*, Proc, Int. Symposium on laser spectroscopy, Los angeles.
- Hu, E.L. and Shaw, D.T. (1998). *Synthesis and assembly*. In *Nanostructure science and technology*, eds. R.W. Siegel, E. Hu, M.C. Roco. Kluwer academic publishers, Dordrecht, The Netherlands.
- Hu, Y., Tung, K.K., Liu, J.P. (2005). *A closer comparison of early and late winter atmospheric trends*. School of Earths Sciences. Georgia institute of technology. Atlanta. Georgia
- Hu, Z., Gerko, O. and Searson, P. C. (2003). Influence of solvent on the growth of ZnO nanoparticles, *Journal of Colloid and Interface Science* 263 (2003) 454–460
- IBM Corporation (2001). *IBM Zurich Research Laboratory: Lab Overview*. [Online]. Available: <http://www.zurich.ibm.com/imagegallery/stm/index2.html>
- Jagadish, C. and Pearton, S. J. (2006). *Zinc Oxide Bulk, Thin Films and Nanostructures Processing, Properties and Application*, Elsevier.
- Jalil, A. A., Triwahyono, S. C., Adam, S. H., Rahim, N. D., Aziz, M. A., Hairom, N. H., Mohamadiah, M. K. (2010). Adsorption of methyl orange from aqueous solution onto calcined Lapindo volcanic mud. *Journal of Hazardous Materials*, 181(3), 755-762. doi:10.1016/j.jhazmat.2010.05.078
- Jiuhui, Q. (2008). Research progress of novel adsorption processes in water purification: A review. *Journal of Environmental Sciences*, 20, 1 – 13.
- Joshi, K.M., and Shrivastava V.S. (2012). Removal of methylene blue dye aqueous solution using photo catalysis, *Int.J.nano Dim*, 2(4): 241-252

- Kansal, S.K., Singh M., Sudc, D. (2006). Studies on photodegradation of two commercial dyes in aqueous phase using different photocatalysts. *J Hazardous material*, in press.
- Kant, S and Kumar A. (2012). Comparative analysis of structural, optical and photocatalytic properties of ZnO prepared by sol-gel method. *VBRI press. India*, 3(4) 350-354
- Kartal, O.E., Erol, M., Oguz, H. (2001).Photo catalytic destruction of phenols by ZnO powders. *Chen Eng Technol.*, 24, 645-649
- Kumar, P.S.S., Sivakumar, R., Anandan, S., Madhavan, J., Maruthamuthu, P.andAshokkumar, M., (2008).Photo-catalytic degradation of Acid Red 88 using Au-TiO₂ nanoparticles in aqueous solutions. *Water Research*, 42, 4878 – 4884.
- Kumar, K.Y., Muralidhara, H.B., Arthoba, N.Y., Balasubramanyam, J. and Hanumanthappa, H. (2013).Hierarchically assembled mesoporous ZnO nanorods for the removal of lead and cadmium by using differential pulse anodic stripping voltammetricmethod. *Powder Technol.* 239: 208–216.
- Kyzas, G. Z., Lazaridis, N. K., & Bikiaris, D. N. (2013). Optimization of chitosan and β -cyclodextrin molecularly imprinted polymer synthesis for dye adsorption. *Carbohydrate polymers*, 91(1), 198-208.
- Langmuir, I. (1920). The octet theory of valence and its applications with special reference to organic nitrogen compounds. *Journal of the American Chemical Society*, 42(2), 274-292.
- Li Y, Xiaodong, L., Junwen, L., Jing, Y. (2005).Photocatalytic degradation of methyl orange by TiO₂ coated with activated carbon, *Catalysis Communications*, 40; 1119-1126
- Lynch, I. and Dawson, K. A. (2008). Protein-nanoparticle interactions.*Nano Today*, 3(1-2).
- Ma, S., Li, R., Lv, C., Xu,W. and Gou, X. (2011).Facile synthesis of ZnO nanorods arrays and hierarchical nanostructures for photocatalysis and gas sensor applications. *J. Hazard. Mater.* 192: 730–740.
- Manahan, S.E. (2000). *Environmental Chemistry* 7thed CRC Press, Boca, Raton FL.

- Maxwell, J. C. (1864). A dynamical theory of the electromagnetic field. Reprinted in WD Niven (Ed.)(1890), *The scientific papers of James Clerk Maxwell* (Vol. 1, pp. 526–597).
- Maynard, A. D. (2007). Nanotechnology: the next big thing, or much ado about nothing?. *Annals of Occupational Hygiene*, 51(1), 1-12.
- Mohan, D. and Pittman, Jr. C. U. (2007). Arsenic removal from water/wastewater using adsorbents-A critical review. *Journal of Hazardous Materials*, 142, 1 – 53.
- Oberdorster, G., Stone, V. and Donaldson, K. (2007). Toxicology of nanoparticles: a historical perspective. *Nanotoxicology*, 1(1), 242 – 254.
- Özgür, Ü, Ya. I., Alivov, C., Liu, A., Teke, M. A., Reshchikov, S., Dogan, V., Avrutin, S. J., Cho, H. and Morkoç, H. (2005). A comprehensive review of ZnO materials and devices. *Journal of applied physics*, 98, 041-301
- Pitcher, S. K., Slade, R. C. T. and Ward, N. I. (2004). Heavy metal removal from motorway stormwater using zeolites, *Sci. Total Environ.* 334–335 161–166.
- Poulis, I. and Tsachpini, J. (1999). Photocatalytic degradation of the textile dye Reactive Orange in the presence of TiO₂ suspensions *Chem Technol Biotechnol*, 74; 349-357
- Rajesh K. N. and Raychaudhuri, A. K. (2013) “Effect of stabilizer on dynamic thermal transport of nanofluids” *Nanoscale Research letters*, 8:125
- Rajeswari, R., and Kanmani, S. (2009). A study on synergistic effect of photocatalytic ozonation for carbaryl degradation. *Desalination*, 242(1), 277-285.
- Rashed, M. N. and El-Amin, A. A. (2007). Photocatalytic degradation of methyl orange in aqueous TiO₂ under different solar irradiation sources. *Int J physical sciences*, 2(3), 73-81
- Roco, M. C. (1999). *Nanotechnology, shaping the world atom by atom*. National Science of technology Council, Committee on Technology, The Interagency Working Group on Nanoscience, Engineering and Technology, Washington D.C., USA.
- Romanchuk, A. Y., Slesarev, A. S., Kalmykov, S. N., Kosynkin, D. V., and Tour, J. M. (2013). Graphene oxide for effective radionuclide removal. *Physical Chemistry Chemical Physics*, 15(7), 2321-2327.
- Samarghandi, M. R., Hadi, M., Moayedi, S., and Askari, F. B. (2009). Two-Parameter Isotherms of Methyl Orange Sorption by Pinecone Derived Activated Carbon. *Iran. J. Environ. Health. Sci. Eng*, 6(4), 285-294.

- Sampa, C., and Biney, K. (2004). *Photo-catalytic degradation of modern textile dyes in waste water using ZnO nanocatalyst*, Kolkata. India.
- Savage, N. and Wentsel, R. (2008). Draft nanomaterial research strategy (NRS). Environmental protection Agency. United States, 1-2.
- Scott, V. D. and Love, G. (1994). *Quantitative Electron Probe Microanalysis*, 2nd edn. Ellis Horwood, Chichester.
- Senthamarai, C., Kumar, P. S., Priyadharshini, M., Vijayalakshmi, P., Kumar, V. V., Baskaralingam, P., and Sivanesan, S. (2013). Adsorption behavior of methylene blue dye onto surface modified *Strychnos potatorum* seeds. *Environmental Progress & Sustainable Energy*, 32(3), 624-632.
- Shanthi S. and Muthuselvi, U. (2012) A study of morphology of synthesized NanoZnO and its application in photodegradation of malachite green dye using different sources of energy 4 39-52
- Shipra, B. (2008). Degradation of methylene blue using ZnS-CdS as photocatalysts. *Int. J. chem Sci* 6(1), 197-204
- Smith, A. (2006). Nanotech - the way forward for clean water? *Filtration and Separation*, 43(8), 32 – 33.
- Sheela, T., Nayaka, Y.A., Viswanatha, R., Basavanna, S. and Venkatesha, T.G. (2012). Kinetics and thermodynamics studies on the adsorption of Zn(II), Cd(II) and Hg(II) from aqueous solution using zinc oxide nanoparticles. *Powder Technol.* 217: 163–170.
- Singh, S., Barick, K. C. and Bahadur, D. (2011). Novel and efficient three dimensional mesoporous ZnO nanoassemblies for environmental remediation. *Int. J. Nanosci.* 10: 1001-1005.
- Soltaninezhad, M. and Aminifar, A. (2011). Study of nanostructures of ZnO as photocatalysts for degradation of organic pollutants. *Int. J. Nano Dim*, 2(2) 137-145
- Sreedhar, S. and Kotaiah, B. (2006). Comparative evaluation of commercial and sewage sludge based activated carbons for the removal of textile dyes from aqueous solutions. *Iran. J. Environ. Health. Sci. Eng.* 3, 239 – 246.

- Taniguchi, N. (1974). On the Basic concept of nano-Technology, proceeding of the international conference on precision Engineering, Tokyo, part mII, Japan society of precision Engineering, 1974
- Tang, W.Z. and Huren, A.N. (1995). UV/TiO₂ photocatalytic oxidation of commercial dyes in aqueous solutions, *Chemosphere*, 31 4157-4170
- Theron, J., Walker, J.A. and Cloete, T.E. (2008). Nanotechnology and Water Treatment: Applications and Emerging Opportunities. *Critical Reviews in Microbiology*, 34, 43 – 69.
- Tokar, E.J., Benbrahim-Tallaa, L. and Waalkes, M.P. (2011). Metal ions in human cancer development. *Metal Ions on Life Science*, 8, 75 – 90.
- United States Environmental Protection Agency (USEPA) (2005). *Guidelines for carcinogen risk assessment* EPA/630/P-03/001F.
- Vieira, C., Morais, S., Ramos, S., Delerue-Matos, C. and Oliveira, M.B.P.P. (2011). Mercury, cadmium, lead and arsenic levels in three pelagic fish species from the Atlantic Ocean: intra- and inter-specific variability and human health risks for consumption. *Food & Chemical Toxicology*, 49; 194 – 200.
- Vijay, M., Anantha, P. and Sreekuma, R, K. (2009). Evolution of photo-catalytic properties of reactive plasma processed nano-crystalline titanium dioxide powder. *Applied Surface Science*, 255, 9316 -9322.
- Wenzhon, S.H., Zhijie, L., Hui, W., Yihang, Z, Qingjie, G. and Yuanli, Z. (2008). Photo catalytic degradation for methylene blue using zinc oxide prepared by codeposition and Sol – gel methods. *Journal of Hazardous materials*, 152; 172 – 175.
- WHO (2006). *Evaluation of certain food additives and contaminants* (Sixty-seventh report of the Joint FAO/WHO Expert Committee on Food Additives). WHO Technical Report Series, No. 940.
- Wu, M.K., Windeler, R.S., Steiner, C.K., Bros, T. and Friedlander, S.K. (1993). Controlled synthesis of nanosized particles by aerosol processes. *Aerosol Science and Technology*, 19, 527 – 548.
- Wu, P.X., Wu, W.M., Li, S.Z. Xing, N. Zhu, N.W, Li, P. Wu, J.H. Yang, C. and Dang, Z. (2009). Removal of Cd²⁺ from aqueous solution by adsorption using Femontmorillonite, *Journal of Hazardous Materials*, 169; 824–830.
- Yantasee, W. Warner, C.L. Sangvanich, T. Addleman, R.S. Carter, T.G, Wiacek, R.J. Fryxell, G.E. Timchalk, C. and Warner, M.G. (2007). Removal of heavy metals

- from aqueous systems with thiol functionalized superparamagnetic nanoparticles, *Environ. Sci. Technol.* 41, 5114–5119.
- Yuan, Q., Li, N., Chi, Y., Geng, W., Yan, W., Zhao, Y., Li, X. and Dong, B. (2013) Effect of large pore size of multifunctional mesoporous microsphere on removal of heavy metal ions. *J. Hazard. Mater.* 254–255: 157–165.
- Zaidi, H. A., and Pant, K. K. (2008). Activity of Oxalic Acid Treated ZnO/CuO/HZSM-5 Catalyst for the Transformation of Methanol to Gasoline Range Hydrocarbons. *Industrial & Engineering Chemistry Research*, 47(2008), 2970 - 2975. doi:10.1021/ie071339y
- Zhang, L., Jiang, Y., Ding, Y., Povey, M. and York, D. (2005). Investigation into the antibacterial behaviour of suspensions of ZnO nanoparticles (ZnO nanofluids). *J. Nanoparticle Res.*, 313, 44 – 51.
- Zhang, J., Fu, D., Xu, Y. and Liu, C. (2010). Optimization of parameters on photocatalytic degradation of chloramphenicol using TiO₂ as photo-catalyst by response surface methodology. *Journal of Environmental Sciences*, 22; 1281 – 1289.
- Zsigmondy, R. (1914). *Colloids and the ultra-microscope*. John Wiley and Sons, NY, USA.
- Zhai, T., Xie, S., Zhao, Y., Sun, X., Lu, X., Yu, M., Xu, M., Xiao, F. and Tong, Y. (2012). Controllable synthesis of hierarchical ZnO nanodisks for highly photocatalytic activity. *CrystEngComm.*, 14: 1850–1855.
- Zhu, C., Wang, L., Kong, L., Yang, X. and Zong, H. (2000). Photocatalytic degradation of azo dyes by TiO₂ in aqueous solution. *Chemosphere*, 41, 303-309

APPENDICES

Appendix I: Effect of variation of contact time on photodegradation of MeO dye under sunlight

<i>Time in Min</i>	<i>Initial Conc</i>	<i>Final Conc</i>	<i>Adsorbed Value</i>
0	30	30	0
30	30	13.36	16.64
60	30	10.48	19.52
90	30	8.36	21.64
120	30	5.53	24.47
150	30	6.69	23.31
180	30	4.34	25.66
210	30	3.23	26.77
240	30	1.21	28.79
270	30	0.81	29.19
300	30	0.54	29.46

Appendix II: Effect of variation of contact time on photodegradation of MeO dye under fluorescent

<i>Time in Min</i>	<i>Initial Conc</i>	<i>Final Conc</i>	<i>Adsorbed Value</i>
0	30	30	0
30	30	15.21	14.79
60	30	11.26	18.74
90	30	10.29	19.71
120	30	8.46	21.54
150	30	6.26	23.74
180	30	5.64	24.36
210	30	4.18	25.82
240	30	2.37	27.63
270	30	1.28	28.72
300	30	1.01	28.99

<i>Final Conc</i>	<i>Adsorbed Value</i>	<i>Ce</i>	<i>Qe</i>	<i>Ce/Qe</i>	<i>Log Ce</i>	<i>Log Qe</i>	<i>Log Ce/qe</i>
30	0		0	0			
13.36	16.64	25.64	416	0.0616	1.408918	2.61909333	0.537941
10.48	19.52	23.91	488	0.0490	1.37858	2.68841982	0.512784
8.36	21.64	8.36	541	0.0155	0.922206	2.73319727	0.337409
5.53	24.47	5.53	611.75	0.0090	0.742725	2.78657398	0.266537
6.69	23.31	6.69	582.75	0.0115	0.825426	2.76548228	0.298475
4.34	25.66	4.34	641.5	0.0068	0.63749	2.80719666	0.227091
3.23	26.77	3.23	669.25	0.0048	0.509203	2.82558838	0.180211
1.21	28.79	1.21	719.75	0.0017	0.082785	2.85718167	0.028974
0.81	29.19	0.81	729.75	0.0011	-0.09151	2.8631741	-0.03196
0.54	29.46	0.54	736.5	0.0007	-0.26761	2.86717275	-0.09333

AppendixIII: Adsorption Langmiur Isotherms Data (Under Sunlight)

<i>Final Conc</i>	<i>Adsorbed Value</i>	<i>Ce</i>	<i>Qe</i>	<i>Ce/Qe</i>	<i>Log Ce</i>	<i>Log Qe</i>	<i>Log Ce/qe</i>
30	0						
15.21	14.79	15.21	369.75	0.041136	1.182129	2.56790818	0.460347
11.26	18.74	11.26	468.5	0.024034	1.051538	2.6707096	0.39373
10.29	19.71	10.29	492.75	0.020883	1.012415	2.69262663	0.375995
8.46	21.54	8.46	538.5	0.01571	0.92737	2.73118571	0.339549
6.26	23.74	6.26	593.5	0.010548	0.796574	2.77342072	0.287217
5.64	24.36	5.64	609	0.009261	0.751279	2.78461729	0.269796
4.18	25.82	4.18	645.5	0.006476	0.621176	2.80989625	0.221067
2.37	27.63	2.37	690.75	0.003431	0.374748	2.83932089	0.131985
1.28	28.72	1.28	718	0.001783	0.10721	2.85612444	0.037537
1.01	28.99	1.01	724.75	0.001394	0.004321	2.86018822	0.001511

Appendix IV: Adsorption Langmuir Isotherms Data (Under Fluorescent Light)

Appendix V: Effect of adsorbent dose on percentage removal of heavy metals

Adsorbent dose (mg)		100		200		300		400		500	
		L ₁	L ₂	L ₁	L ₂	L ₁	L ₂	L ₁	L ₂	L ₁	L ₂
% Removal	Cd	82.8	82.9	84.1	84	88.3	88	93.5	93.5	93.2	94.4
	Ni	83	83.1	83.6	83.5	89.1	89	94	94	94.0	94.6
	Cu	84.1	84	86.4	85	91.4	92	92.7	92.7	92.5	93.3

Appendix VI: Effect of initial concentration of heavy metals

Heavy metals initial (mgL ⁻¹)		100		200		300		400	
		L ₁	L ₂	L ₁	L ₂	L ₁	L ₂	L ₁	L ₂
Removal %	Cd	83.1	83.2	66.8	66.5	62	62.2	59	60
	Ni	82.9	83	63.4	63.5	61.8	62	60.1	60.9
	Cu	83	83	66.6	66.7	62.2	61.9	59.4	59.5

Appendix VII: Effect of pH

pH		2		4		6		8	
		L ₁	L ₂	L ₁	L ₂	L ₁	L ₂	L ₁	L ₂
Removal %	Cd	28.5	30	44	43	82.3	84	92.1	93
	Ni	29.1	31	43.8	43.2	82.3	83.2	92.8	93
	Cu	26.5	27.2	45.1	44	82.9	83	92	94.1

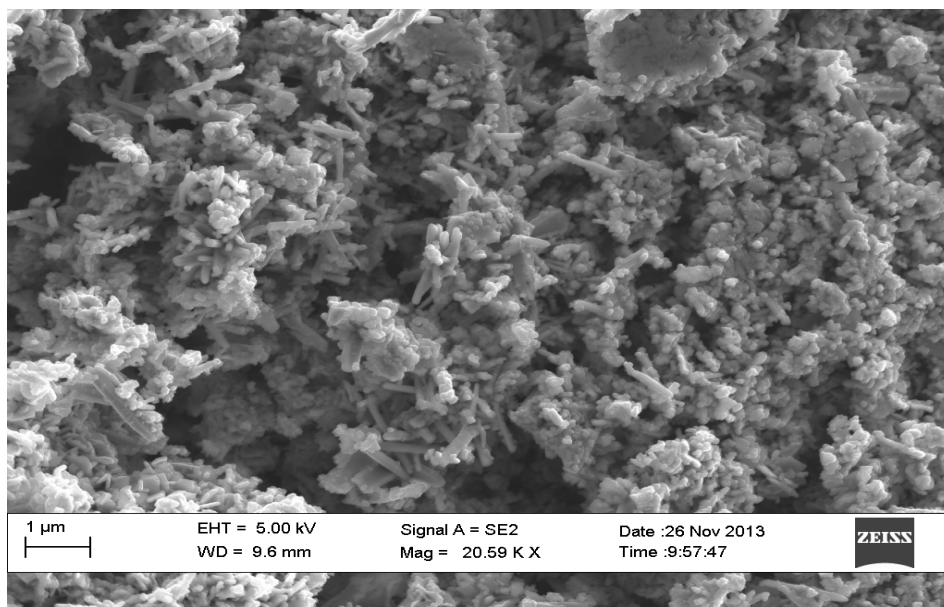
Appendix VIII: Lagergren Adsorption Kinetics Data (Under Sunlight)

Qt	$Qe-Qt$	$\log(Qe-Qt)$	t/Qt
4.36	411.64	2.614518	3.2101
6.09	481.91	2.682966	3.9917
21.64	519.36	2.715468	4.158965
24.47	587.28	2.768845	4.903964
23.31	559.44	2.747754	6.435006
25.66	615.84	2.789468	7.014809
26.77	642.48	2.80786	7.844602
28.79	690.96	2.839453	8.336228
29.19	700.56	2.845445	9.249743
29.46	707.04	2.849444	10.1833

Appendix IX: Lagergren Adsorption Kinetics Data (Under Fluorescent)

Qt	$Qe-Qt$	$\log(Qe-Qt)$	t/Qt
14.79	354.96	2.550179	2.028398
18.74	449.76	2.652981	3.201708
19.71	473.04	2.674898	4.56621
21.54	516.96	2.713457	5.571031
23.74	569.76	2.755692	6.31845
24.36	584.64	2.766889	7.389163
25.82	619.68	2.792167	8.13323
27.63	663.12	2.821592	8.686211
28.72	689.28	2.838396	9.401114
28.99	695.76	2.842459	10.3484

Appendix X: Observed SEM diagram ZnO nanorods, L₁ at low magnification (Mag 20.59 K)



Appendix XI: Observed SEM diagram L₂ at Low Magnification (Mag 20.66 K)